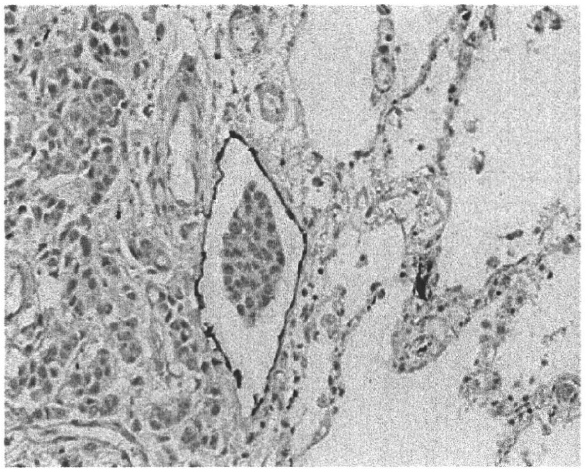

Fig. 5b Histopathological Findings of the Lung Metastasis (D2-40 stain, high magnification)

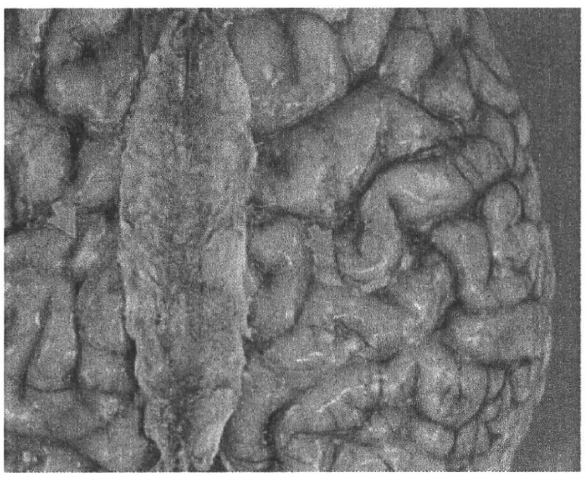

Fig. 5c Autopsy Appearance of the Brain Metastases (arrows)

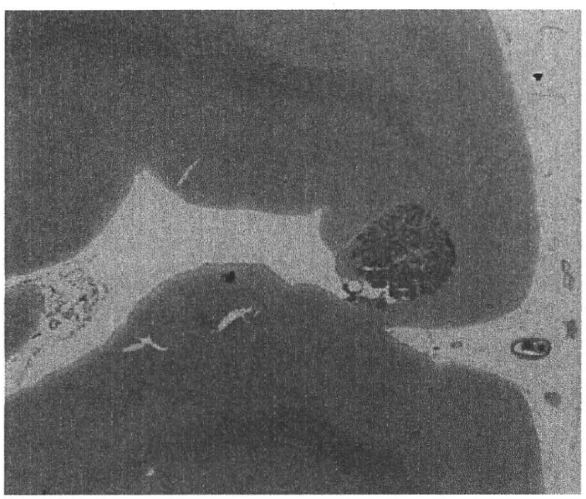

Fig. 5d Histopathological Findings of the Brain Metastasis (H-Estain, low magnification)

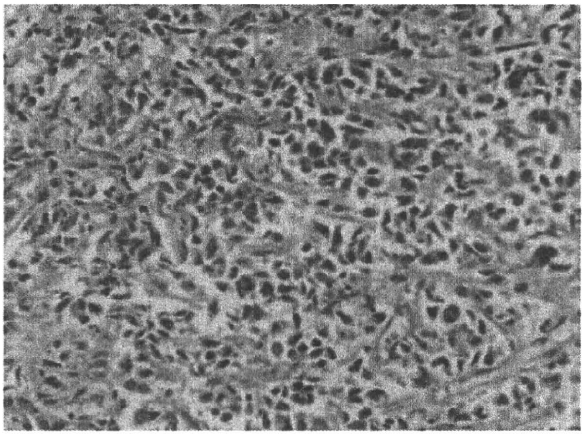

Fig. 5e Histopathological Findings of the Liver Metastasis (H-Estain, high magnification)

節，腸骨動脈周囲リンパ節への転移を認めた。

肺では肉眼的に数 mm 大の転移性白色結節と，その周囲に網状の白色線条（**Fig. 5a**）を認め，癌性リンパ管症を示唆するものであった。また組織学的にも，血管内への腫瘍細胞の浸潤も認めるものの，リンパ管内への腫瘍細胞の浸潤が優位であり（**Fig. 5b**），組織学的にも癌性リンパ管症を示唆していると考えた。さらに大脳，小脳への多発転移巣はいずれも脳回の表層に沿って存在し（**Fig. 5c**），解剖学的血行路とは無関係に存在していた。病理組織学的にいずれの転移巣も大脳皮質表層または脳室に接して存在していた（**Fig. 5d**）。また組織学的に，肝臓や膵臓，肺門リンパ節，下腿皮膚の各転移巣では，腫瘍細胞は原発巣に比べ小型化し，明るい胞体は消失して核の異型性もより強くなった紡錘形の腫瘍細胞（**Fig. 5e**）が主体であった。なお，これらの腫瘍細胞は消化 PAS 染色には陰性であったが，CEA 染色には陽性であった。

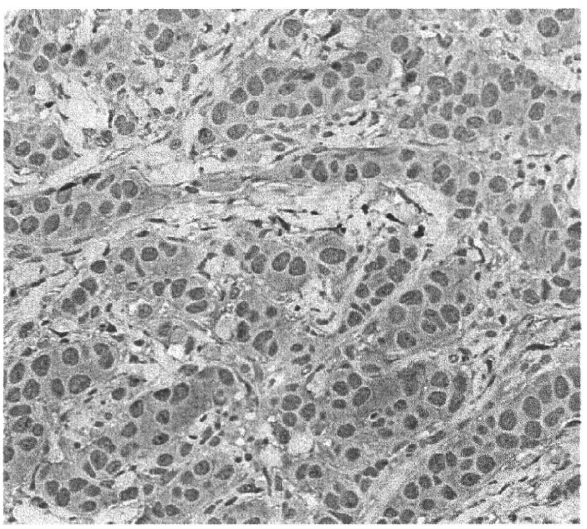

Fig. 6 CXCR4 Expression (red) in Invasive Paget Cells

また副病変として肺うっ血，胸水貯留（右：1,000 ml，左900 ml），腹水貯留（600 ml），うっ血腎，大動脈粥状硬化症などが認められた。なお剖検所見から重複癌は認めなかった。

考　　察

乳房外 Paget 病の多くは表皮内癌として緩徐に進行するが，Paget 細胞が基底膜を破り，間質に浸潤した Paget 癌となると比較的早期に転移を来たし，治療に難渋することが多い。自験例も初診時にすでに多発性リンパ節転移と骨転移をきたしており，種々の治療を行ったものの初診から約1年9ヶ月後に永眠した。今回は化学療法として，低用量 FP および ADR や，TXT 単独療法，FECOM 療法，GEM 療法などを施行した。低用量 FP および ADR においては明らかな有効性を認めたものの，他については明確な有効性は認められなかった。現在のところ遠隔転移を生じた乳房外 Paget 癌に対して明確な有効性をもった化学療法は確立されておらず，消化器癌や乳癌に用いられてきた抗癌剤が単独もしくは併用で試みられているにすぎない。吉野[1]らは複数個の所属リンパ節転移を有する症例に対して，リンパ節を郭清して術後 FECOM 療法を中心に補助化学療法を施行した6例と，施行しなかった4例を比べ，遠隔転移までの平均期間はそれぞれ15ヶ月と6.5ヶ月であったと報告し，同様に FECOM 療法また低用量 FP 療法が有効であったとの報告[2~4]などが存在するものの，症例数が少なく現在なお有効性が確立されているものはないのが現状である。

永松[5]らは乳房外 Paget 病の100例の検討において，浸潤癌症例では高率にリンパ節転移をきたし，リンパ節転移例13例中11例は腫瘍死したと報告しており，自験例を含めてリンパ節転移例は予後不良と言わざるを得ない。さらに浸潤癌では病理組織学的にリンパ管や血管の内腔に腫瘍細胞が浮遊もしくは充満する所見がしばしば見受けられる[6]とされるが，自験例でも原発巣の紅斑部および結節部ともにリンパ管内への浸潤像を確認した。これは，乳房外 Paget 癌はリンパ行性優

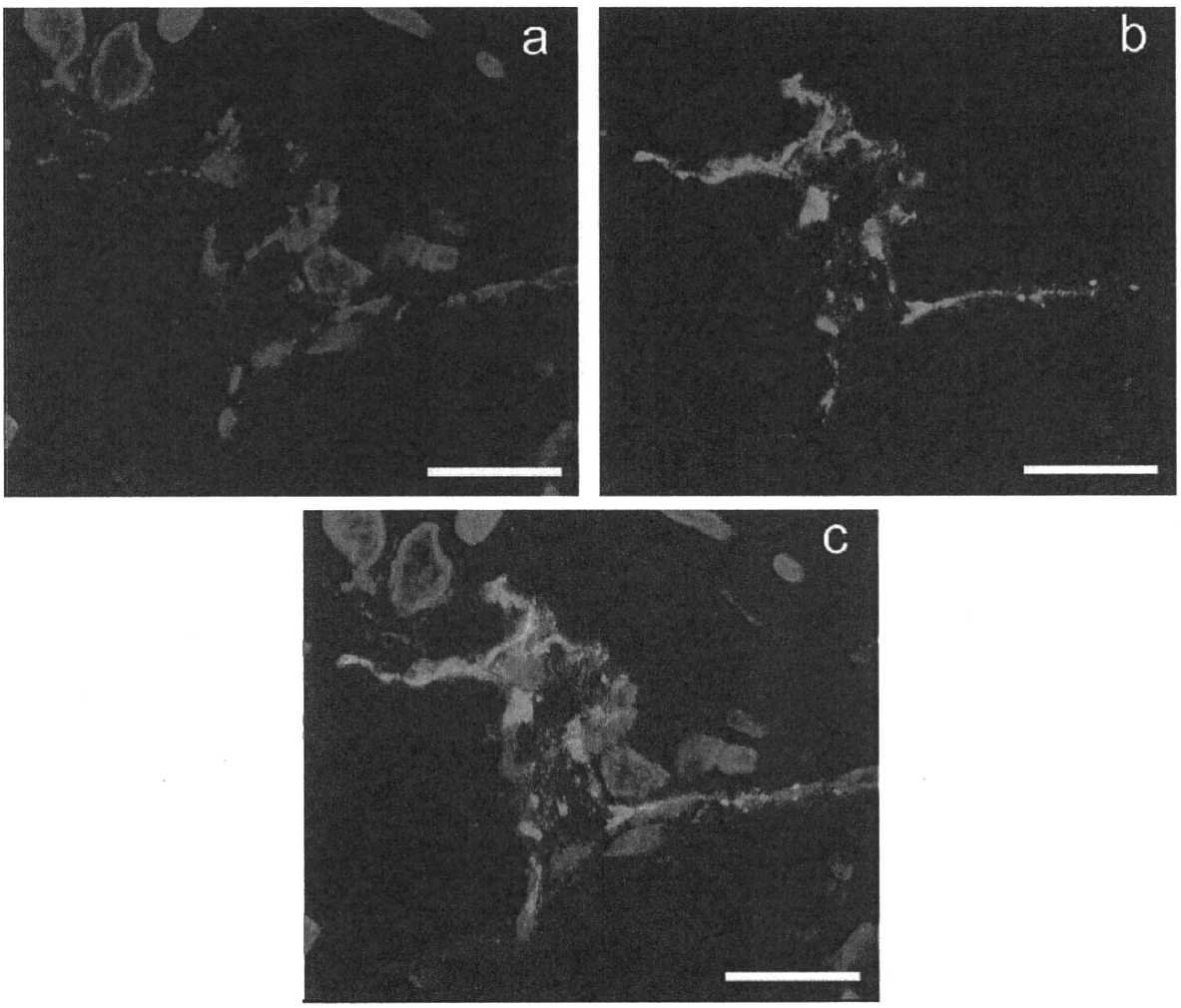

Fig. 7　a–c: Immunofluorescence staining shows SDF-1 (red) expression in lymphatic vessels (green). Nuclei are stained blue (DAPI stain). Scale bars = 20 μm

位に転移が進行していくと考察される報告[1,7,8]と合致する所見であり，一方で粘着性に富む[9]ことからリンパ管内に腫瘍塞栓を引き起こし，「パンツ型浸潤」と呼ばれる下腹から鼠径，大腿への逆行性皮膚転移[10]をきたすものと考えられる。また近年，平川[11]らはPaget細胞がCXCR4を発現している症例では高率にリンパ節転移がみられ，生存率が有意に低いことを報告し，腫瘍のCXCR4とリンパ管のstromal cell-derived factor（SDF-1）との親和性がリンパ管浸潤を促進させると報告している。自験例でもCXCR4染色をおこなったところ，浸潤するPaget細胞にはCXCR4の発現を認め（**Fig. 6**），さらにリンパ管でのSDF-1の発現が確認できた（**Fig. 7A～C**）。

次に原発巣紅斑部では腫瘍細胞は病理組織学的に淡明な胞体を有する大型の類円形細胞であったが，結節部では好酸性に染まり明瞭な核小体をもつ細胞となり，各転移巣においては小型のより異型性の強い紡錘形の細胞が主体（**Fig. 5e**）で，腫瘍の進展に伴い細胞形態の変化を認めた。CEA染色はいずれの腫瘍細胞も陽性で染色性の相違を認めなかったが，PAS染色は原発巣紅斑部の上皮内にとどまる腫瘍細胞のみが陽性であった。これらの所見は腫瘍細胞が進展するに伴って，より未分化な性質へと変化し，基底膜を超えて浸潤した段階から粘液癌的性質は消失していることを示唆[12]していると考えた。

我々は剖検を行うことで，大脳，小脳，下垂体，肝臓，胆嚢，両肺，脾臓，両側副腎，左下肢皮膚転移，また頸椎から仙骨までの多発性骨転移と骨髄，肋骨，骨盤骨転移，さらに肺門リンパ節，膵頭部周囲リンパ節，傍大動脈リンパ節，腸骨動脈周囲リンパ節への転移が確認されたが，下垂体，胆嚢，脾臓，副腎，骨髄への転移は，剖検にて初めて判明した転移巣であり，生前施行したPET-CTやMRI，エコー等の画像検査ではこれらの転移巣は確認できなかった。

我々は腫瘍の転移様式を考える上で，肺，脳転移に注目した。肺の剖検時の肉眼的所見では，転移巣である白色の多発結節を認めると同時に，白色の網状線条（**Fig. 5a**）を多数認めた。これらは肺での癌性リンパ管症を肉眼的に示唆する所見であったと考える。さらに肺転移巣である白色結節を病理組織学的に検討すると，腫瘍細胞の脈管への浸潤像がみられ，血管よりもリンパ管優位に腫瘍細胞による閉塞像（**Fig. 5b**）が認められた。したがって組織学的にも癌性リンパ管症をうかがわせる所見が得られた。自験例では2009年4月より両側の胸水が出現していたが，同年4月6日に施行したCTでは網目状の陰影を認めるのみで，結節状の肺転移巣は認めず，後のCTにて結節状の転移巣を確認した。これらは乳房外Paget病の肺転移においては，画像上まず線状や網目状の陰影として認められ，進行すると胸水の貯留をきたすとする熊野[13]らの報告と一致する。また並川[8]らは4例の乳房外Paget病の剖検例を報告している。それによれば肺転移の初発臨床所見として，全例が胸水もしくは画像上の網状影やスリガラス陰影が先行したと報告されており，自験例も含めて乳房外Paget病の肺転移では，結節状の転移巣の出現より胸水や癌性リンパ管症など，リンパ管の閉塞に伴う症状が先行する特徴があるのではないかと推測される。

次に脳転移に注目すると，剖検時の肉眼的所見では転移巣である多数の白色の結節は大脳皮質表面の脳回陥凹部と，脳室に接する部分に偏在していた（**Fig. 5c**）。病理組織学的にみても，転移巣は脳脊髄液と接する大脳皮質表在もしくは脳室に接して存在しており（**Fig. 5d**），転移巣の分布は解剖学的血行路とは一致せず，血行性転移よりも脳脊髄液を介して転移が進展したのではないかと考えられた。さらに自経例では2008年9月より連日，絞扼性の頭痛とふらつきを認めるようになり，同年10月と12月に頭部のMRIを施行しているものの転移巣は確認できず，このときの髄液細胞診はclass IIであった。症状出現から5ヶ月後の2009年3月の頭部のMRIにて初めて，左前頭葉皮質と右尾状核にそれぞれ3 mmと4 mmの脳転移を疑う所見が確認された。したがって髄液細胞診はclass IIではあったが，頭痛やふらつきといった症状の先行は，脳転移巣によるものではなく，腫瘍により脳脊髄液の循環路に障害をきたし，頭蓋内圧亢進症を来たしたことが原因ではないかと推察され，これらの事を踏まえると，脳への転移様式も血行性転移よりは脊椎へ転移した後に髄腔播種をきたし，脳脊髄液を介して転移が進展したのではないかと考えられた。

乳房外Paget病の転移臓器では領域リンパ節が最も多く，次いで肝，肺，骨，副腎とされており[14]，脳転移例はまれである。我々が調べた限り，本症の脳転移例は自験例を含めて本邦で過去に5例[7,8,15]の報告がある。金子[7]らは遠隔転移を来した陰部Paget病を中心に191例の検討を行い，脳転移例は1.5%に過ぎなかったと報告している。実際，剖検や開頭をされているケースは極めて少数であり実数を示しているかは不明である。しかし自験例でも，頭部の造影MRIで脳転移巣は径3 mmの段階で的確に描出されており，開頭しなくても画像的に十分脳転移の有無の把握は可能であると考えられる。これらを踏まえると本症の脳転移例の実数は極めて少数であると推察され，それは本症の転移が血行性よりもむしろリンパ行性優位に進展しやすいことが一因ではないかと考えた。

本稿の要旨は第416回日本皮膚科学会大阪地方会にて発表した。

引用文献

1. 吉野公二，山崎直也，山本明史，並川健二郎，吉田寿斗志：乳房外パジェット病の進展様式および化学療法について．日皮会誌　2006；116：1339-1342
2. 山崎直也：これまでにおこなわれた進行期乳房外Paget病の治療の総括とそこから見えてくるもの．Skin Cancer　2008；23：341-346
3. 徳田安孝，小口真司，山崎百合子：5-FUとCDDPの低濃度持続投与法（low dose FP療法）が奏功した進行期乳房外Paget病の3例．日皮会誌　1997；107：21-27
4. Kariya K, Tsuji T, Schwartz RA: Trial of low-dose 5-fluorouracil/cisplatin therapy for advanced extramammary Paget's disease. Dermatol Surg　2004; 30: 341-344
5. 永松将吾，中岡啓喜，村上信司，橋本公二：愛媛大学皮膚科における乳房外Paget病100例の検討．Skin Cancer　2009；24：30-34
6. 大原國章，大西泰彦，川端康浩：乳房外Paget病の診断と治療．Skin Cancer　1993；8：39-60
7. 金子　聡，佐藤勘治，富田昌宏，他：脳転移を来した乳房外Paget病の1例．日皮会誌　2004；114：1287-1291
8. 並川健二郎，山崎直也，山本明史，他：乳房外Paget病の剖検例．Skin Cancer　2006；21：199-205
9. 南光弘子，渥美令子，市原健一，他：術中突然死をみた外陰部Paget病の心転移例．日皮会誌　1987；97：1181-1188
10. 村田洋三，熊野公子，伴　政雄：パンツ型の浸潤をきたした皮膚悪性腫瘍の4例．Skin Cancer　1998；3：83-87
11. Hirakawa S, Detmar M, Kerjaschki D, et al: Nodal lymphangiogenesis and metastasis: Role of tumor-induced lymphatic vessel activation in extramammary Paget's disease. Am J Pathol　2009; 175 (5): 2235-2248
12. 市川雅子，村木良一，大塚藤男，中村靖司，小形岳三郎，野本岩尾：外陰部Paget癌の剖検例．臨皮　1994；48：103-106
13. 熊野公子，村田洋三：Paget癌の肺転移の特徴．Skin Cancer　1990；5：80-84
14. Helwig EB, Graham JH: Anogenital (extramammary) Paget's disease. A clinicopathological study. Cancer　1963; 16: 387-403
15. 野手とし子，鶴田和仁，俵　哲，荒木淑郎，指宿一彦：脳血管障害様症状で発症した乳房外Paget病の1剖検例．臨床神経学　1982；22：621-627

An Autopsy Case of Extramammary Paget's Carcinoma with Brain Metastases and Analysis of the Progress Patterns

Takashi Yamanaka, Atsushi Tanemura, Eriko Iimuro, Megumi Nishioka, Tomoko Yajima, Mamori Tani, Mari Wataya-Kaneda and Ichiro Katayama

Department of Dermatology, Course of Integrated Medicine
Graduate School of Medicine, Osaka University
2-2, Yamadaoka, Suita, Osaka 565-0871, Japan

Satoshi Nojima and Katsuyuki Aozasa

Department of Pathology, Course of Integrated Medicine
Graduate School of Medicine, Osaka University
2-2, Yamadaoka, Suita, Osaka 565-0871, Japan

Satoshi Hirakawa and Koji Hashimoto

Department of Dermatology, Ehime University Graduate School of Medicine
Shitsukawa, Toon, Ehime 791-0295, Japan

Key words: *extramammary Paget's carcinoma, brain metastasis, autopsy, lymphogenous metastasis*

We report an autopsy case of Paget's Carcinoma with brain metastases. A 72-year-old man presented with irregular erythema consisting of hyper- and hypo-pigmented macule and ulcerated red nodule on the left inguinal region. He was diagnosed with Paget's carcinoma by skin biopsy. The biopsy specimen showed numerous lymphatic ducts fulfilled with Paget cells in the dermis. ^{18}F-FDG-PET-CT examination demonstrated multiple metastases to lymph nodes and bones superior to the inguinal region.

Initially, multiple metastatic lesions seemed to disappear after several courses of chemotherapy. However, the tumors recurred and metastasis spread to the brain within 1 year after initiating comprehensive treatment.

An autopsy was performed with written informed consent from the family and these findings suggest how Paget cells metastasized especially to the lung and brain in this patient.
Skin Research, 9: 229–236, 2010

Leukemia Research xxx (2011) xxx–xxx

Contents lists available at ScienceDirect

Leukemia Research

journal homepage: www.elsevier.com/locate/leukres

Predictability of the response to tyrosine kinase inhibitors via *in vitro* analysis of Bcr-Abl phosphorylation

Masaru Shibata[a], Sachiko Ezoe[a,*], Kenji Oritani[a], Keiko Matsui[a], Masahiro Tokunaga[a], Natsuko Fujita[a], Yuri Saito[a], Takayuki Takahashi[b], Masayuki Hino[c], Itaru Matsumura[d], Yuzuru Kanakura[a]

[a] *Hematology and Oncology, Osaka University, Graduate School of Medicine, 2-2 Yamada-oka, Suita, Osaka 565-0871, Japan*
[b] *Kobe City Medical Center General Hospital, Kobe, Japan*
[c] *Department of Hematology, Graduate School of Medicine, Osaka City University, Osaka, Japan*
[d] *Department of Internal Medicine, Kinki University School of Medicine, Sayama, Japan*

ARTICLE INFO

Article history:
Received 16 December 2010
Received in revised form 12 January 2011
Accepted 14 January 2011
Available online xxx

Keywords:
CML
Tyrosine kinase inhibitor
Bcr-Abl
Crkl
Phosphorylation
Immunoblot

ABSTRACT

It would be of great value to predict the efficacy of tyrosine kinase inhibitors (TKIs) in the treatment of individual CML patients. We propose an immunoblot system for detecting the phosphorylation of Crkl, a major target of Bcr-Abl, in blood samples after *in vitro* incubation with TKIs. When the remaining phosphorylated Crkl after treatment with imatinib was evaluated as the "residual index (RI)", high values were found in accordance with imatinib resistance. Moreover, RI reflected the outcome of imatinib- as well as second generation TKIs with a high sensitivity and specificity. Therefore, this system should be useful in the selection of TKIs.

1. Introduction

The introduction of tyrosine kinase inhibitors (TKIs) targeting Bcr-Abl have dramatically improved the treatment of CML. Imatinib mesylate (Gleevec; Novartis Pharmaceuticals, East Hanover, NJ) was shown to induce high rates of cytogenetic and molecular responses, resulting in greatly prolonged survival in CML patients [1,2]. However, despite the remarkable improvement in survival and responsiveness with imatinib-treatment, a considerable proportion of the patients treated with imatinib have been reported to exhibit either primary or secondary resistance or intolerance [3–5]. Clinical resistance to imatinib can result from mutations in the Abl kinase domain at residues that directly contact imatinib or that influence imatinib binding [6]. As resistance can also arise in the absence of Bcr-Abl mutations, other mechanisms of resistance and disease progression may exist, including Bcr-Abl-independent signaling in CML cells [7]. To overcome the resistance and intolerance to imatinib, efforts have been made to develop second- and third-generation TKIs. Examples of such inhibitors include nilotinib (Tasigna, Novartis) [8], dasatinib (Sprycel, Bristol-Myers Squibb) [9] and other TKIs under clinical investigation such as bosutinib [10] and INNO-406 [11]. These TKIs are significantly more potent than imatinib and have exhibited efficacy against many types of imatinib-resistant Bcr-Abl mutants. Furthermore, they are also candidates for first-line therapy, as there is a need to improve the results achieved with imatinib [12–14]. In parallel with the entrance of new therapeutic compounds, an important question is which TKI is the most appropriate to each CML patient.

To establish a system with which we can predict the response of each patient to TKIs, we investigated in this study the phosphorylation of Crkl, a major target of Bcr-Abl, after *in vitro* incubation with or without TKIs in peripheral blood (PB) samples from patients either newly diagnosed or resistant to imatinib. It is demonstrated that this *in vitro* analysis system is highly reflective of the clinical response to TKIs of CML patients, and these data should prove useful in selecting TKIs in individual cases.

2. Patients, materials and methods

2.1. Patient blood samples

Thirty-one patients with CML in the chronic phase (CP) were included in this study (Table 1). The optimal response, response and resistance were defined in accordance with the European Leukemia Net (ELN) recommendations [15,16]. Briefly, an "optimal response" to imatinib means achieving a complete hematological response (CHR) at 3 months or complete cytogenetic response (CCyR) at

* Corresponding author. Tel.: +81 6 6879 3871; fax: +81 6 6879 3879.
E-mail address: sezoe@bldon.med.osaka-u.ac.jp (S. Ezoe).

0145-2126/$ – see front matter © 2011 Elsevier Ltd. All rights reserved.
doi:10.1016/j.leukres.2011.01.012

6 months after the induction of imatinib, and resistance means failure to achieve such a response. On the other hand, in nilotinib- or dasatinib-treated patients, a "response" means a minor cytogenetic response (mCyR) at 3 months or partial cytogenetic response (PCyR) at 6 months after the induction of the second generation TKI, and resistance means failure to achieve this response.

Ten microliters of the PB samples were obtained from patients with informed consent at the beginning or before the initiation of imatinib, nilotinib or dasatinib. Half of each sample was used for examination of the Bcr-Abl sequence, which was performed by the SRL Co. (Tokyo, Japan), and the other half was used for immunoblot analysis.

Approvals for the study were obtained from the institutional review boards of all the participating facilities.

2.2. Reagents

Imatinib, methanesulfonate salt was kindly provided by Novartis Pharmaceuticals (Basel, Switzerland), and nilotinib and dasatinib were purchased from LC laboratories (Boston, MA). The antibodies used in this study were as follows: anti-Lyn, anti-phospho-Crkl, anti-phospho-c-Abl from Cell Signaling Technology (Beverly, MA), anti-phospho-Lyn(Y396) from Epitomics (Burlingame, CA), anti-Crkl, anti-β-actin from Santa Cruz Biotechnology (Santa Cruz, CA), and the secondary antibodies, anti-Rabbit IgG HRP and anti-Goat IgG HRP were from Promega (Madison, WI). Pervanadate was purchased from Sigma–Aldrich (St. Louis, MO).

2.3. Cell line

A Bcr-Abl positive human cell line, K562, was used in the preliminary experiments in this study. K562 cells were maintained in RPMI1640 (nacalai tesque, Kyoto, Japan) supplemented with 10% fetus bovine serum (FBS) (EQUITECH-BIO, Kerrville, TX).

2.4. Immunoblot assays of patients' samples

Whole blood cell samples from patients were used within 3 h after blood had been drawn. Red cells were lysed with Whole Blood Lysing Reagents (Beckman Coulter, Brea, CA), and white blood cells were cultured with or without imatinib, nilotinib or dasatinib. After 5-h incubation, the cell lysates were collected and subjected to immunoblot assays. Gel electrophoresis and immunoblot assays were performed according to methods described previously [17,18]. Immunoreactive proteins were visualized with an enhanced chemiluminescence detection system (PerkinElmer Life Sciences, Boston, MA).

2.5. Evaluation of phosphorylation intensity and determination of the "residual index (RI)"

The intensity of each blot of immunoreactive protein was quantified using ChemiDoc XRS+ with Image Lab Software (Bio Rad, Tokyo Japan). The RI values of each patient to TKIs were determined in accordance with the numerical expression, as indicated in Fig. 2A.

2.6. Statistical analysis

Analysis of variance was used to assess data reproducibility. The Mann–Whitney rank sum was used to define differences between groups.

3. Results

3.1. Immunoblot analysis of phosphorylated Crkl in CML patients

To assess the drug response of the CML patients, we performed immunoblot assays detecting phosphorylated Crkl, a direct target of Bcr-Abl kinase. To establish the experimental procedures, preliminary experiments were performed with K562, a CML blast crisis cell line, or blood sample from a newly diagnosed CML patient (Patient A), 98% of whose PB cells were Bcr-Abl-positive on fluorescence *in situ* hybridization (FISH). First, to determine the optimum incubation period for the TKIs, PB cells were incubated with or without TKIs for varying time periods. A two-hour incubation was not sufficient because imatinib did not completely suppress the phosphorylation of Crkl, while 24-h incubation was too long because the PB neutrophils appeared to die (Fig. 1A, left panel). A five-hour incubation completely eliminated the phosphorylation of Crkl without cell death. On the other hand, simultaneous treatment with a phosphatase inhibitor sustained the phosphorylation of Crkl even after treatment for 24 h (Fig. 1A, right panel). Thus, we decided to incubate cells for 5 h without phosphatase inhibitors. Next, to build an *in vitro* simulation model for the estimation of the activities of TKIs in the body, we fixed the concentrations of TKIs at the peak value of plasma concentrations in patients (Cmax) after administration of the recommended dose of TKIs. The Cmax of imatinib in CML patients after taking orally 400 mg of the drug is 3.0–4.8 μM, and that of nilotinib after taking 400 mg is 2.9–4.0 μM. In the case of

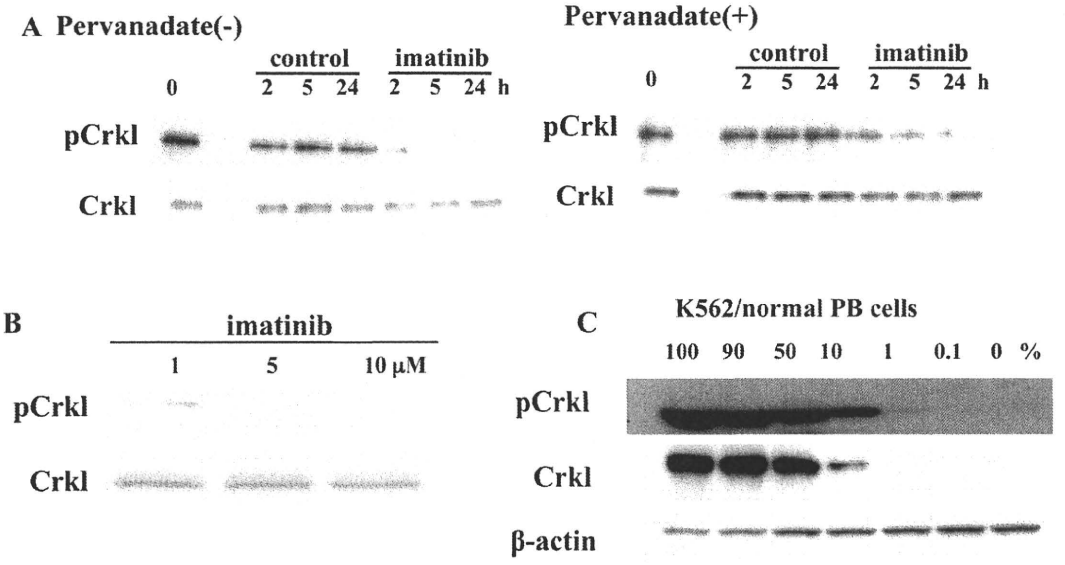

Fig. 1. Optimization of western blot after TKI-incubation. (A and B) Blood sample from Patient A was incubated with or without 5 μM imatinib supplemented with (right panel) or without (left panel) 10 μM of pervanadate for the indicated periods (A) or incubated with imatinib at the indicated concentrations for 5 h (B). The treated cells were lysed and subjective to immunoblot analysis using the indicated antibodies. (C) K562 cells were mixed into normal human PB cells at the indicated ratios. Then the samples were subjective to immunoblot analysis.

Please cite this article in press as: Shibata M, et al. Predictability of the response to tyrosine kinase inhibitors via *in vitro* analysis of Bcr-Abl phosphorylation. Leuk Res (2011), doi:10.1016/j.leukres.2011.01.012

dasatinib, the Cmax after the ingestion of 100 mg dasatinib was 100nM [19–21]. In terms of pharmacokinetics, we fixed the concentrations of these TKIs (imatinib, nilotinib and dasatinib) at 5 μM, 5 μM, and 0.1 μM, respectively. As shown in Fig. 1B, 1 μM of imatinib did not eliminate the phosphorylation of Crkl in the examined sample of patient A who are newly diagnosed and well responded to imatinib, but 5 μM and 10 μM of imatinib did, indicating that 1 μM is too low concentration for estimation of clinical outcome. Finally, to estimate the sensitivity of this system, K562 cells were mixed with normal PB cells at variable ratios, as indicated. Fig. 1C shows that the phosphorylated Crkl at the lowest 1% was detectable in K562 cells. Thus, we analyzed patients having more than 10% Bcr-Abl-positive cells in PB by FISH.

3.2. Immunoblot analysis

To quantify the *in vitro* responsiveness to TKIs, we measured the density of each blot using a densitometric method. We then defined "residual index (RI)" for each TKI by the numerical expression as shown in Fig. 2A. Triplicate measurements were performed on 3 individual patients (Patient B, C and D). There were no significant variations among the RIs in each patient. Standard error for each sample set was less than 5% (4.6%, 1.2% and 3.4%, respectively) (Fig. 2B).

3.3. Responses to the TKIs in patients with various stages of CML

Fig. 3A represents typical results of the immunoblot analyses in 2 patients with newly diagnosed CML (Patient 1 and 2), and 2 patients who were receiving imatinib but were displaying resistance (Patient 16 and 17). Although all of these samples exhibited apparent phosphorylation of Crkl without TKIs, the phosphorylated Crkl disappeared from the samples of Patients 1 and 2 when incubated with imatinib, nilotinib or dasatinib. In the case of Patients 16 and 17, on the other hand, weak bands remained in the imatinib and/or nilotinib-incubated samples, but disappeared in the dasatinib-treated ones. Thus, this immunoblot analysis appeared to be useful in evaluating Crkl phosphorylation after *in vitro* TKI-incubation. All patients were divided into two groups: one being newly diagnosed and another receiving imatinib-therapy but showing resistance. The imatinib-RIs of the samples from the imatinib-resistant group (median RI: 34.2%) were much higher than those of the samples from newly diagnosed patients (median RI: 4.2%) (Fig. 3B).

3.4. Sequential examinations using the residual index

RI values were analyzed sequentially in the course of the different TKI-treatments in 2 imatinib-resistant patients (Patient 23 and 27).

Patient 23 (Fig. 4A): after six months of treatment with imatinib, the drug was changed to dasatinib because of a failure to achieve an optimal response (72% $Ph1^+$ in FISH). Six months after the start of dasatinib, $Ph1^+$ cells were disappeared. The samples were obtained twice: prior to the treatment with imatinib, and at the time of change to dasatinib. Immunoblot analysis showed that neither imatinib nor nilotinib eliminated the phosphorylation of Crkl at the initiation of treatment, but dasatinib did. Furthermore the RI values were under 10% only in the sample incubated with dasatinib.

Patient 27 (Fig. 4B): when the first sample was obtained, the percentage of $Ph1^+$ cells was 93% after 7-year treatment with imatinib.

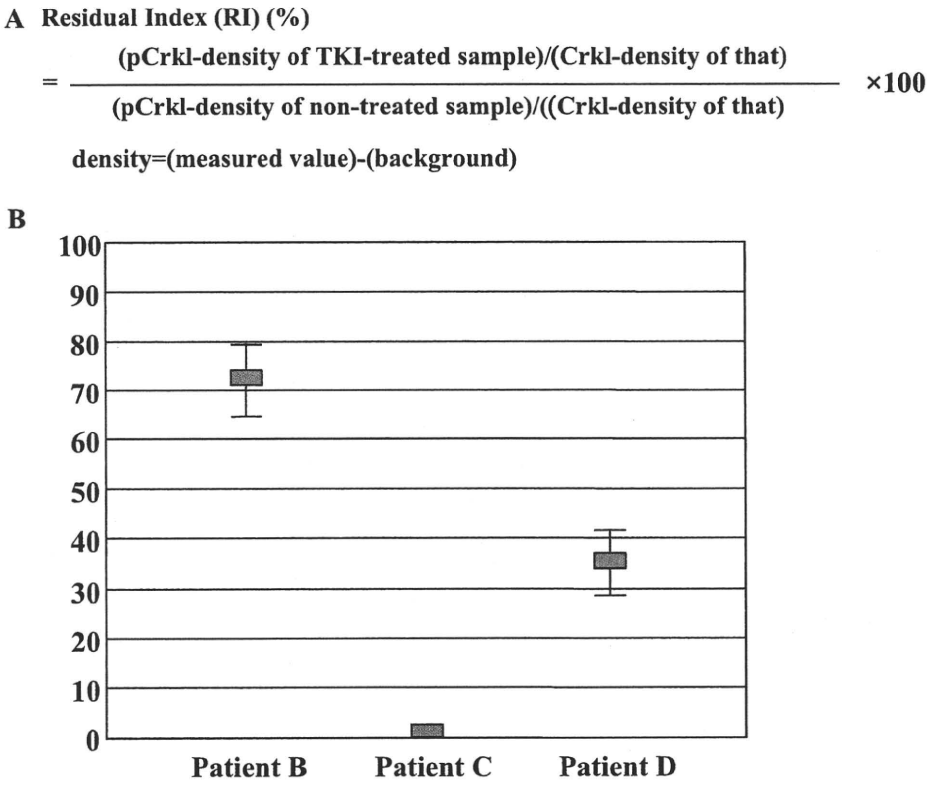

Fig. 2. "Residual index (RI)". (A) The numerical expression of RI. "Measured value" means the density of each blot measured by densitometric method. (B) The reproducibility of RIs for imatinib treatment. Means and standard errors, representing triplicate assays in 3 patients, are shown.

Please cite this article in press as: Shibata M, et al. Predictability of the response to tyrosine kinase inhibitors via *in vitro* analysis of Bcr-Abl phosphorylation. Leuk Res (2011), doi:10.1016/j.leukres.2011.01.012

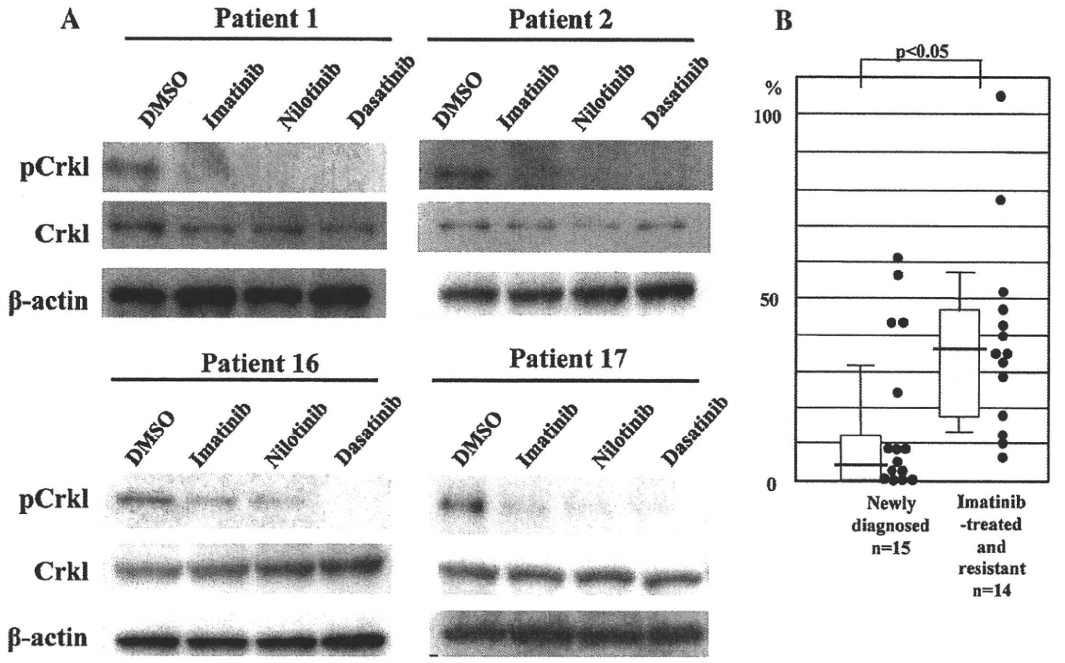

Fig. 3. Different RI values against imatinib between patients at diagnosis and patients showing imatinib-resistance. (A) Four typical data of immunoblots were represented. PB cells from newly diagnosed patients (Patient 1 and 2) or patients (Patient 16 and 17) who had been receiving imatinib-therapy but showed its resistance were incubated for 5 h *in vitro* with or without indicated TKIs. The concentration of imatinib, nilotinib, and dasatinib are 5 μM, 5 μM, and 0.1 μM, respectively. The incubated cells were lysed and subjected to immunoblot analysis using the indicated antibodies. (B) RIs against imatinib were calculated in 15 patients at diagnosis and 14 patients who had been receiving imatinib-therapy and showed its resistance. The distribution of RIs in each group was plotted. Representative box plots show values within the 25th to 75th percentile. Medians are indicated in crossbar. Fifth and 95th percentiles are shown by error bars. The statistical difference was $p < 0.05$.

Then the treatment was changed to dasatinib, which was stopped because of a strong pancytopenia. The patient was then treated with nilotinib, but the percentage of $Ph1^+$ cells again increased. The second sample was obtained at the time of the change from dasatinib to nilotinib. In both samples, the incubation with the three TKIs did not eliminate the phosphorylation of Crkl. Although the second sample exhibited a strong sensitivity only to dasatinib (RI = 4.1%), the remaining CML cells additionally displayed continuous Lyn-phosphorylation (Fig. 4B).

3.5. RIs in patients with Bcr-Abl point mutations

The most important issue in TKIs resistance is the acquisition of point mutations in Bcr-Abl. Bcr-Abl mutations were detected in 4 samples (Table 2). The RI values of Patient 28, with a threonine-to-isoleucine mutation at codon 315 (T315I), were higher than 10% in all the TKI-treated samples. In accordance with the *in vitro* results, the disease was refractory to both imatinib and dasatinib. A phenylalanine-to-leucine mutation at codon 317 (F317L) and a methionine-to-threonine at codon 351 (M351T) were detected in Patient 27. F317L is reported to confer high responsiveness to nilotinib, while M351T does the same to dasatinib. The RI values of this patient were over 10% in all of the samples treated with TKIs, which conformed the outcome of failing to achieve CHR after nilotinib or dasatinib treatment. Next, the RI value in the sample with the phenylalanine-to-valine mutation at codon 359 (F359V) (Patient 23) was less than 10% only in the dasatinib-treated sample, which does not conflict with the reported IC50 data. Finally, although the F317L mutation is reported to be highly sensitive to nilotinib, the RI value for nilotinib in Patient 19, who later proved to be resistant to nilotinib but responded to dasatinib, was higher than 10%, and lower than 10% for dasatinib. Therefore, RIs are likely to be highly correled with the favorability of Bcr-Abl mutations to TKIs, and in some cases, to predict the responsiveness with higher sensitivity than mutations.

3.6. Correlation of RI with patient outcome

To analyze whether the RIs correlate with the clinical response to TKIs, newly diagnosed patients ($n = 15$) were separated into two groups in accordance with the most recent outcome, imatinib-sensitive ($n = 13$), who achieved an optimal response after the sample collection, and imatinib-resistant ($n = 2$), who did not. The median RI of the patients in the sensitive group was 4.2% and that in the resistant group was 43.2% ($p < 0.05$) (Fig. 5, left panel). We also assessed the predictability of the response to nilotinib. Eight patients imatinib resistant had undergone nilotinib-therapy. Among them, 4 achieved optimal responses and the others failed. The median RI in the nilotinib-sensitive group was 3.5% in contrast to 31.2% in the resistant group (Fig. 5, middle panel). Although the sample size was too small to conduct statistical analysis, the RIs were clearly separated between dasatinib-sensitive and -resistant groups (Fig. 5, right panel).

When the cut-off value of RI was set at 10%, the specificities, sensitivities and predicted values were all 100% in terms of nilotinib and dasatinib responsiveness (Table 3). Also, in the evaluation of imatinib-treatment, the specificity and sensitiveness were more than 77%. Therefore, it is suggested that the RIs (cut-off value: 10%) are useful as a novel predictor for clinical utility of TKIs, especially in imatinib-resistant cases.

4. Discussion

Imatinib, the first approved TKI for CML, frequently induces durable cytogenetic remission and thus occupies an important position as the current standard of care. Now, second-generation

Please cite this article in press as: Shibata M, et al. Predictability of the response to tyrosine kinase inhibitors via *in vitro* analysis of Bcr-Abl phosphorylation. Leuk Res (2011), doi:10.1016/j.leukres.2011.01.012

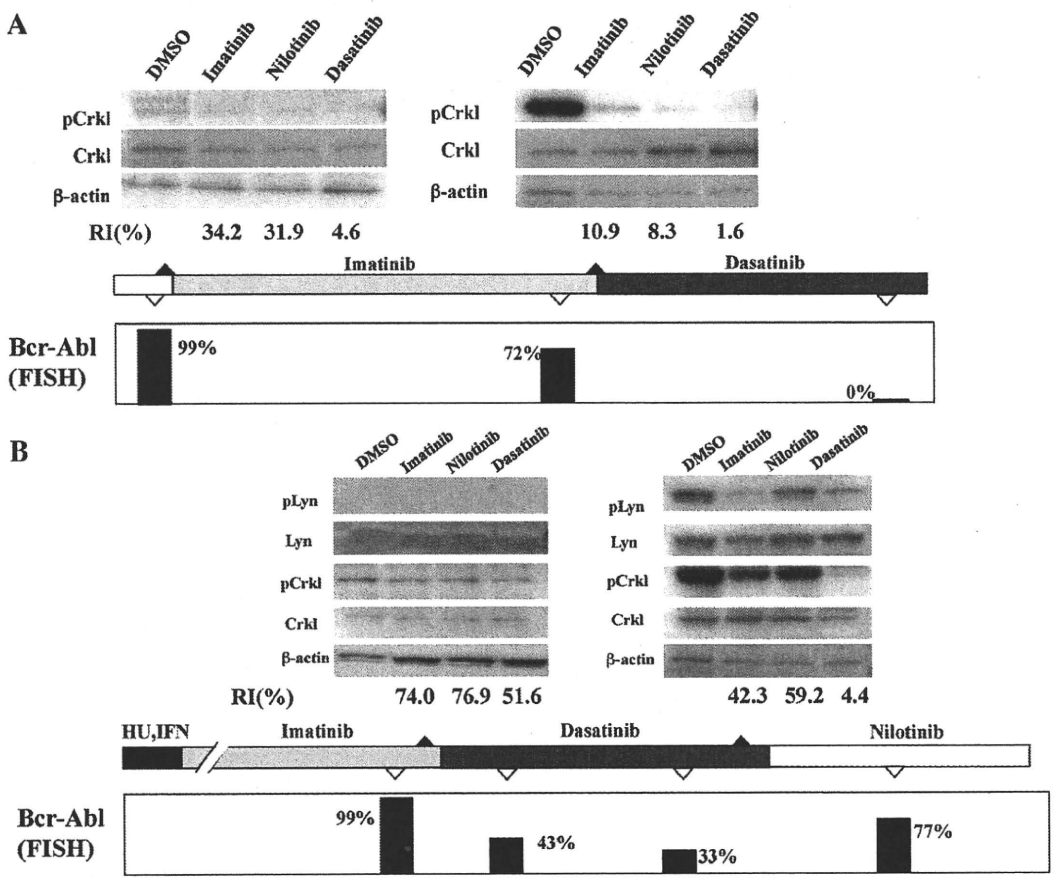

Fig. 4. Sequential examinations of RI values during clinical treatments in two patients. Immunoblots were sequentially analyzed during CML-treatment in two patients who showed resistance to TKIs. Data of immunoblots using the indicated antibodies are shown with their clinical course. FISH analyses are indicated by open triangles, and immunoblot analysis by closed triangles.

Table 1
Patient characteristics.

Characteristic	
No. of patients	31
Median age, y (range)	55 (20–89)
Sex (male/female)	14/17
Treatment before sample collection	
No	13
IFN	3
TKI	18
Bcr-Abl mutation	4
Median follow-up, months (range)	6 (3–14)

TKIs, such as nilotinib and dasatinib, have now been made available [12,13]. Although these TKIs are significantly more potent and show higher sensitivity against some imatinib-resistant mutations, there are no useful guidelines for the proper choice of second-generation TKIs in imatinib-resistant patients. Furthermore, second-generation TKIs have recently been recommended as first-line therapies based on the evidence that an earlier achievement of remission may provide a better clinical outcome or less disease progression. There is still a need for indicators pointing to the proper drug choice for individual patients. The *in vitro* responsiveness to TKIs in terms of cell proliferation has been demonstrated to be a predictor of clinical response. The IC50, a cell based screen for resistance determining the drug concentration that can induce 50% of growth suppression, is a potent predictor of the responsiveness to drugs. In patients with *de novo* CML, the $IC50^{imatinib}$ was reported to possess a high predictive value [22]. However, determination of the IC50 for each TKI requires so much effort and time that an application suitable for all patients may be quite a distant prospect. Furthermore, as the optimal concentration varies for each TKI, comparing the efficacy between different TKIs is difficult. Although the cellular IC50 s for the effect of TKIs on Bcr-Abl point mutations have been reported [23–26], this information

Table 2
Patients with BCR-ABL mutations, and their RI values.

Patient	Mutation	RIs			Clinical outcome
		Imatinib	Nilotinib	Dasatinib	
Patient 19	F317L	40.0	30.8	3.9	Imatinib and nilotinib resistant, and dasatinib respond
Patient 23	F359V	15.8	11.9	1.4	Imatinib resistant, and nilotinib and dasatinib intolerant
Patient 27	M351T/F317L	74.0	76.9	51.6	imatinib resistant, and nilotinib and dasatinib intolerant
Patient 28	T315I	104.2	88.0	93.0	Imatinib and dasatinib resistant

Please cite this article in press as: Shibata M, et al. Predictability of the response to tyrosine kinase inhibitors via *in vitro* analysis of Bcr-Abl phosphorylation. Leuk Res (2011), doi:10.1016/j.leukres.2011.01.012

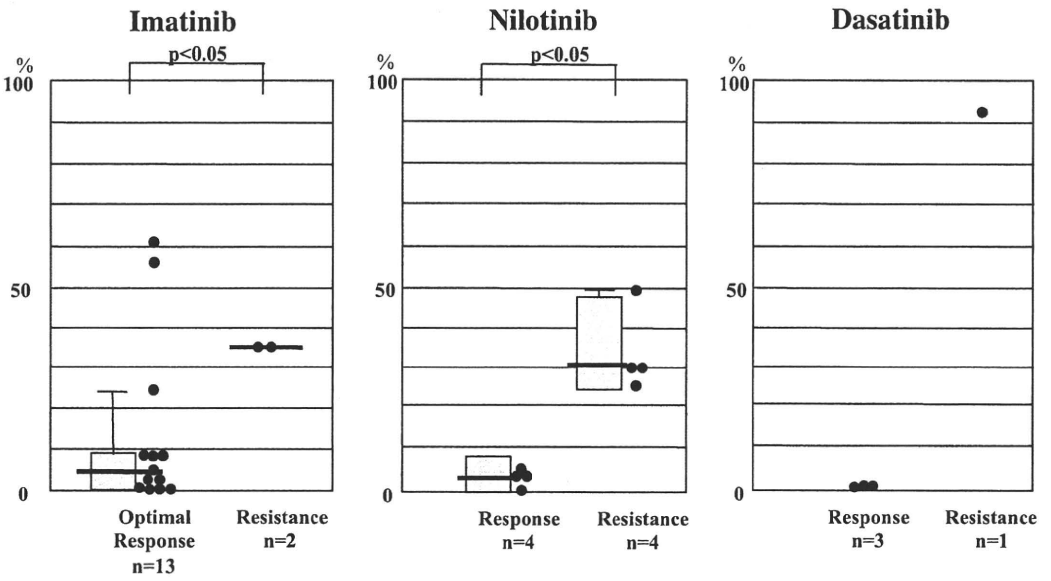

Fig. 5. RI values in patients grouped by clinical response to each TKI-therapy. Fifteen patients were newly diagnosed as CML, and their PB cells were obtained just before the beginning of imatinib-therapy. The patients were divided into two groups: "optimal response" in imatinib-treated patients means *de novo* CML patients who later proved to achieve optimal response, and "Resistance" means patients who later failed to achieve optimal response. Among 12 patients who had showed imatinib-resistance, 8 patients received nilotinib-therapy and 4 patients received dasatinib-therapy at a stretch of imatinib-therapy. Their PB cells were obtained just before the change of therapy. The patients were divided into two groups: that of responsive patients and of resistant patients to each TKI. Dot plots demonstrate the RI values of patients to each TKI. Representative box plots show values within the 25th to 75th percentile. Medians are indicated in crossbar. Fifth and 95th percentiles are shown by error bars.

Table 3
Sensitivity and specificity.

	Optimal response	Resistance	Predicted value
Newly diagnosed and Imatinib-treated patients ($n = 15$)			
RI < 10	10	0	100%
RI ≥ 10	3	2	40%
Specificity/sensitivity	77%	100%	
Imatinib-resistant and Nilotinib-treated patient ($n = 8$)			
RI<10	4	0	100%
RI ≥ 10	0	4	100%
Specificity/sensitivity	100%	100%	
Imatinib-resistant and Dasatinib-treated patients ($n = 4$)			
RI < 10	3	0	100%
RI ≥ 10	0	1	100%
Specificity/sensitivity	100%	100%	
	Newly diagnosed and later achieved optimal response	Imatinib-treated and showed resistance to Imatinib	Predicted value
All included and evaluable patients ($n = 27$)			
RI < 10	10	1	91%
RI ≥ 10	3	13	81%
Specificity/sensitivity	77%	93%	

is only useful when the mutated subclone is the predominant cell population.

In this study, we evaluated the effect of TKIs on Crkl phosphorylation as a "residual index". It is noteworthy that the samples from patients who had shown resistance to imatinib had much higher RIs than the samples from newly diagnosed patients. In the case of newly diagnosed patients, most samples responsive to imatinib *in vitro*, but two patients whose samples displayed markedly high RIs *in vitro* proved not to achieve an optimal response to the drug. Although substantial accordance was later detected in the immunoblot data between the responsiveness and resistance to imatinib, a few samples had markedly high RIs in patients who later achieved optimal responses to imatinib. These exceptional cases will have to be followed for a longer period. The data showed 100% of sensitivity and 77% of specificity when the RIs were separated at 10%. On the other hand, in imatinib-resistant patients, the results of the tests did reflect the patient outcome. Although the sample size was small, the immunoblot analysis was able to predict the clinical responsiveness to nilotinib or dasatinib treatment with 100% sensitivity and specificity. Thus, this system can be a useful tool for selecting TKIs, especially in imatinib-resistant patients. It may be inferred that the lower confidence in

Please cite this article in press as: Shibata M, et al. Predictability of the response to tyrosine kinase inhibitors via *in vitro* analysis of Bcr-Abl phosphorylation. Leuk Res (2011), doi:10.1016/j.leukres.2011.01.012

the case of the untreated patients might due to a multiplicity of CML subclones.

CML patients develop imatinib resistance through either Bcr-Abl dependent or independent mechanisms. The most characterized and frequent mechanism is the acquisition of point mutations within the kinase domain of the Bcr-Abl gene, and some of the mutations such as T315I are potent predictors for outcome. However, even in those patients who have some mutations other than a few restricted mutations such as T315I and F317L, we cannot accurately predict the efficacy of TKIs. Furthermore, nearly half of the patients resistant to imatinib have no mutations in Bcr-Abl, which indicates that other mechanisms are also important for the acquisition of drug-resistance. Thus, we need other information for selecting TKIs. In this study, 4 patients carried point mutations in this region. Samples from 3 of them had RI values compatible with the predictive outcomes from the mutations. Notably, the RI values of the other sample contradicted the response of the mutation, but accorded with the actual response of the patient. From these points of view, the system described here can be utilized as another powerful predictor than IC50s for Bcr-Abl mutations.

The immunoblot system described here has the capacity to detect TKI-resistant subclones, including CML cells with Bcr-Abl mutations. In addition, our strategy seems to evaluate Bcr-Abl activity more directly than the cellular IC50 and require smaller population of TKI-resistant subclones than Bcr-Abl sequence analysis. Thus, when used together with the cellular IC50 values and Bcr-Abl sequence, this immunoblot system should help improve the treatment of patients with CML.

Conflict of interest

The authors state that they have no conflict of interest.

Acknowledgements

We would like to thank Shibano M. (Sakai Munincipal Hospital, Sakai, Japan), Sugahara H. (Sumitomo Hospital, Osaka, Japan), Moriyama Y. (Ikeda City Hospital, Ikeda, Japan), Azenishi Y. (Minoh City Hospital, Minoh, Japan), Ishida N. (Itami City Hospital, Itami, Japan), and Yamada M. (Suita Munincipal Hospital, Suita, Japan), who kindly provided blood samples.

References

[1] Kantarjian H, Sawyers C, Hochhaus A, Guilhot F, Schiffer C, Gambacorti-Passerini C, et al. Hematologic and cytogenetic responses to imatinib mesylate in chronic myelogenous leukemia. N Engl J Med 2002;346:645–52.
[2] O'Brien SG, Guilhot F, Larson RA, Gathmann I, Baccarani M, Cervantes F, et al. Imatinib compared with interferon and low-dose cytarabine for newly diagnosed chronic-phase chronic myeloid leukemia. N Engl J Med 2003;348:994–1004.
[3] Sawyers CL, Hochhaus A, Feldman E, Goldman JM, Miller CB, Ottmann OG, et al. Imatinib induces hematologic and cytogenetic responses in patients with chronic myelogenous leukemia in myeloid blast crisis: results of a phase II study. Blood 2002;99:3530–9.
[4] Talpaz M, Silver RT, Druker BJ, Goldman JM, Gambacorti-Passerini C, Guilhot F, et al. Imatinib induces durable hematologic and cytogenetic responses in patients with accelerated phase chronic myeloid leukemia: results of a phase 2 study. Blood 2002;99:1928–37.
[5] Druker BJ, Sawyers CL, Kantarjian H, Resta DJ, Reese SF, Ford JM, et al. Activity of a specific inhibitor of the BCR-ABL tyrosine kinase in the blast crisis of chronic myeloid leukemia and acute lymphoblastic leukemia with the Philadelphia chromosome. N Engl J Med 2001;344:1038–42.
[6] Azam M, Latek RR, Daley GQ. Mechanisms of autoinhibition and STI-571/imatinib resistance revealed by mutagenesis of BCR-ABL. Cell 2003;112:831–43.
[7] Donato NJ, Wu JY, Stapley J, Gallick G, Lin H, Arlinghaus R, et al. BCR-ABL independence and LYN kinase overexpression in chronic myelogenous leukemia cells selected for resistance to STI571. Blood 2003;101:690–8.
[8] Weisberg E, Manley PW, Breitenstein W, Bruggen J, Cowan-Jacob SW, Ray A, et al. Characterization of AMN107, a selective inhibitor of native and mutant Bcr-Abl. Cancer Cell 2005;7:129–41.
[9] Talpaz M, Shah NP, Kantarjian H, Donato N, Nicoll J, Paquette R, et al. Dasatinib in imatinib-resistant Philadelphia chromosome-positive leukemias. N Engl J Med 2006;354:2531–41.
[10] Boschelli DH, Wu B, Ye F, Wang Y, Golas JM, Lucas J, et al. Synthesis and Src kinase inhibitory activity of a series of 4-[(2,4-dichloro-5-methoxyphenyl)amino]-7-furyl-3-quinolinecarbonitriles. J Med Chem 2006;49:7868–76.
[11] Kimura S, Naito H, Segawa H, Kuroda J, Yuasa T, Sato K, et al. NS-187, a potent and selective dual Bcr-Abl/Lyn tyrosine kinase inhibitor, is a novel agent for imatinib-resistant leukemia. Blood 2005;106:3948–54.
[12] Saglio G, Kim DW, Issaragrisil S, le Coutre P, Etienne G, Lobo C, et al. Nilotinib versus imatinib for newly diagnosed chronic myeloid leukemia. N Engl J Med 2010;362:2251–9.
[13] Kantarjian H, Shah NP, Hochhaus A, Cortes J, Shah S, Ayala M, et al. Dasatinib versus imatinib in newly diagnosed chronic-phase chronic myeloid leukemia. N Engl J Med 2010;362:2260–70.
[14] Wei G, Rafiyath S, Liu D. First-line treatment for chronic myeloid leukemia: dasatinib, nilotinib, or imatinib. J Hematol Oncol 2010;3:47–56.
[15] Baccarani M, Saglio G, Goldman J, Hochhaus A, Simonsson B, Appelbaum F, et al. Evolving concepts in the management of chronic myeloid leukemia: recommendations from an expert panel on behalf of the European LeukemiaNet. Blood 2006;108:1809–20.
[16] Baccarani M, Rosti G, Castagnetti F, Haznedaroglu I, Porkka K, Abruzzese E, et al. Comparison of imatinib 400 mg and 800 mg daily in the front-line treatment of high-risk, Philadelphia-positive chronic myeloid leukemia: a European LeukemiaNet Study. Blood 2009;113:4497–504.
[17] Tokunaga M, Ezoe S, Tanaka H, Satoh Y, Fukushima K, Matsui K, et al. BCR-ABL but not JAK2 V617F inhibits erythropoiesis through the Ras signal by inducing p21CIP1/WAF1. J Biol Chem 2010;285:31774–82.
[18] Ezoe S, Matsumura I, Nakata S, Gale K, Ishihara K, Minegishi N, et al. GATA-2/estrogen receptor chimera regulates cytokine-dependent growth of hematopoietic cells through accumulation of p21(WAF1) and p27(Kip1) proteins. Blood 2002;100:3512–20.
[19] Tanaka C, Yin OQ, Sethuraman V, Smith T, Wang X, Grouss K, et al. Clinical pharmacokinetics of the BCR-ABL tyrosine kinase inhibitor nilotinib. Clin Pharmacol Ther 2010;87:197–203.
[20] Peng B, Hayes M, Resta D, Racine-Poon A, Druker BJ, Talpaz M, et al. Pharmacokinetics and pharmacodynamics of imatinib in a phase I trial with chronic myeloid leukemia patients. J Clin Oncol 2004;22:935–42.
[21] Luo FR, Yang Z, Camuso A, Smykla R, McGlinchey K, Fager K, et al. Dasatinib (BMS-354825) pharmacokinetics and pharmacodynamic biomarkers in animal models predict optimal clinical exposure. Clin Cancer Res 2006;12:7180–6.
[22] White D, Saunders V, Lyons AB, Branford S, Grigg A, To LB, et al. In vitro sensitivity to imatinib-induced inhibition of ABL kinase activity is predictive of molecular response in patients with de novo CML. Blood 2005;106:2520–6.
[23] von Bubnoff N, Schneller F, Peschel C, Duyster J. BCR-ABL gene mutations in relation to clinical resistance of Philadelphia-chromosome-positive leukaemia to STI571: a prospective study. Lancet 2002;359:487–91.
[24] von Bubnoff N, Veach DR, Miller WT, Li W, Sanger J, Peschel C, et al. Inhibition of wild-type and mutant Bcr-Abl by pyrido-pyrimidine-type small molecule kinase inhibitors. Cancer Res 2003;63:6395–404.
[25] von Bubnoff N, Veach DR, van der Kuip H, Aulitzky WE, Sanger J, Seipel P, et al. A cell-based screen for resistance of Bcr-Abl-positive leukemia identifies the mutation pattern for PD166326, an alternative Abl kinase inhibitor. Blood 2005;105:1652–9.
[26] O'Hare T, Walters DK, Stoffregen EP, Sherbenou DW, Heinrich MC, Deininger MW, et al. Combined Abl inhibitor therapy for minimizing drug resistance in chronic myeloid leukemia: Src/Abl inhibitors are compatible with imatinib. Clin Cancer Res 2005;11:6987–93.

Please cite this article in press as: Shibata M, et al. Predictability of the response to tyrosine kinase inhibitors via *in vitro* analysis of Bcr-Abl phosphorylation. Leuk Res (2011), doi:10.1016/j.leukres.2011.01.012

European Journal of Haematology 86 (412–419)

ORIGINAL ARTICLE

Presence of B-cell clones in T-cell lymphoma

Mona A.A. Zaki[1], Naoki Wada[1], Masaharu Kohara[1], Junichiro Ikeda[1], Yumiko Hori[1], Shigeki Fujita[1], Hiroyasu Ogawa[2], Haruo Sugiyama[3], Masayuki Hino[4], Yuzuru Kanakura[5], Eiichi Morii[1], Katsuyuki Aozasa[1]

[1]Department of Pathology, Osaka University Graduate School of Medicine, Suita, Osaka; [2]Department of Internal Medicine, Hyogo College of Medicine, Nishinomiya, Hyogo; [3]Department of Functional Diagnostic Science, Osaka University Graduate School of Medicine, Suita, Osaka; [4]Department of Clinical Hematology and Diagnostics, Osaka City University Graduate School of Medicine, Osaka; [5]Department of Hematology and Oncology, Osaka University Graduate School of Medicine, Suita, Osaka, Japan

Abstract

Objectives: The presence of B-cell clones in 76 cases with peripheral T-cell lymphoma (PTCL) and precursor T-lymphoblastic lymphoma (T-LBL) and its correlation with Epstein–Barr virus (EBV) was studied. *Methods:* DNA was extracted from paraffin sections and/or fresh-frozen samples and then used for clonality analysis using a modified BIOMED-2 polymerase chain reaction (PCR)-based method. *Results:* T- and B-cell clones were detected in 59 (77.6%) and 14 (18.4%) of 76 patients, respectively: 90% and 30% of cases with PTCL, not otherwise specified, 76.4% and 17.6% of cases with angioimmunoblastic T-cell lymphoma, 77% and 7.6% of cases with adult T-cell lymphoma, 50% and 0% of cases with anaplastic large T-cell lymphoma, 62.5% and 12.5% of cases with T-LBL, and 50% and 0% of cases with intestinal T-cell lymphoma, respectively. Histological and immunohistochemical analyses revealed the presence of large B cells in lesional tissues, which were occasionally monoclonal. The presence of B-cell clones was highly associated with EBV positivity, as revealed by *in situ* hybridization. In two cases that were evaluated by serial histological and molecular examination, EBV-positive cells persisted in one and disappeared in the other. *Conclusions:* These findings suggest a role for EBV in the evolution of B-cell clones in T-cell lymphomas.

Key words T-cell lymphoma; B-cell clone; polymerase chain reaction; immunohistochemistry; Epstein–Barr virus

Correspondence Katsuyuki Aozasa, MD, PhD, Department of Pathology (C3), Osaka University Graduate School of Medicine, 2-2 Yamadaoka, Suita, Osaka 565-0871, Japan. Tel: 81-6-6879-3710; Fax: 81-6-6879-3713; e-mail aozasa@molpath.med.osaka-u.ac.jp

Accepted for publication 24 February 2011 doi:10.1111/j.1600-0609.2011.01597.x

Peripheral T-cell lymphomas are a heterogeneous group of tumors representing approximately 7% of all non-Hodgkin's lymphomas, according to a large international survey (1). In the World Health Organization (WHO) classification of lymphoid neoplasms, each disease is classified based on the combined findings of clinical features and morphological, immunohistochemical, and genotypical findings. However, diagnosis of PTCL remains difficult because a polymorphous pattern of proliferation containing varying numbers of inflammatory cells occurs frequently, potentially masking the neoplastic nature of the disease. Under such conditions, molecular analysis for detection of clonal proliferation of T-lymphoid cells is a prerequisite to confirm the diagnosis for these cases. Thus, clonality analysis with a polymerase chain reaction (PCR)-based method is considered to be reliable for detection of both T- and B-cell clones (2, 3).

Recently, the presence of B-cell clones that frequently contain Epstein–Barr virus (EBV) genomes was reported in cases of PTCL, particularly among cases of PTCL, not otherwise specified (PTCL-NOS) and angioimmunoblastic T-cell lymphoma (AITL) (4–8). Immunodeficient conditions that evolved during the courses of these lymphomas may be responsible for this phenomenon. However, the clinical significance of this phenomenon as well as its behavior and course has not yet been clarified because of very limited information.

In this study, various types of PTCL and precursor T-lymphoblastic lymphoma (T-LBL) were analyzed for the presence of B-cell clones using a modified PCR-based method with paraffin-embedded and fresh-frozen samples. Subsequently, the association with EBV, the histomorphology of the lesions, clinical findings (including the presence of immunodeficient conditions), and outcomes were evaluated.

Materials and methods

Patients

Between November 1999 and February 2009, 4162 patients were registered with the Osaka Lymphoma Study Group (OLSG), Osaka, Japan. Histological specimens obtained by biopsy were fixed in 10% formalin and routinely processed for paraffin embedding. Histological sections (4 μm) were cut and stained with hematoxylin and eosin and then were subjected to a standard avidin–biotin complex immunoperoxidase procedure. All the histological sections were reviewed by one of the authors (KA) and then were classified according to the WHO classification system. The diagnosis of malignant lymphoma was confirmed in 3307 (79.5%) of 4162 cases. Of these 3307 cases, 3031 (91.7%) were non-Hodgkin's lymphoma (NHL) and 276 (8.3%) were Hodgkin's lymphoma. The T-cell lymphoma cases consisted of 558 (16.9%) cases of NHL, 241 cases of PTCL-NOS, 64 cases of AITL, 80 cases of adult T-cell leukemia/lymphoma (ATL), 47 cases of anaplastic large-cell lymphoma (ALCL), 31 cases of T-LBL, and 12 cases of intestinal T-cell lymphoma (ITL). Initially, the most recent 197 cases (77 PTCL-NOS, 30 AITL, 38 ATL, 35 ALCL, 11 T-LBL, and six ITL cases) were retrieved, and then DNA was extracted from their paraffin blocks. In total, 76 cases (30 PTCL-NOS, 17 AITL, 13 ATL, six ALCL, eight T-LBL, and two ITL cases), from which DNA with >300 bp was available for analysis, were selected; fresh-frozen tissues were available in 14 of these cases. Clinical data for these cases are summarized in Table 1.

Immunohistochemistry (IHC)

Monoclonal antibodies used for IHC were CD20, CD79a, CD3, CD8, CD30, CD21, and ALK (Dakocytomation, Glostrup, Denmark; diluted at 1 : 400, 1 : 100, 1 : 50, 1 : 100, 1 : 50, 1 : 100, and 1 : 50, respectively), CD4 (1 : 40; Novocastra Laboratories, Newcastle, UK), CD10 (used as a prediluted antibody; Nichirei Biosciences, Tokyo, Japan), and programmed cell death 1 (PD-1; 1 : 50; Abcam, Tokyo, Japan). Immunohistochemistry was performed using an automated staining system (Dako Autostainer; DakoCytomation, Glostrup, Denmark).

In situ hybridization (ISH)

ISH using an Epstein–Barr virus-encoded small RNA (EBER) probe was performed to examine the presence of the EBV genome using formalin-fixed paraffin-embedded sections with the EBER DAB application kit (DakoCytomation).

Clonality analysis for B and T cells

One to five 4- to 10-μm-thick sections were cut from the paraffin-embedded samples, deparaffinized with xylene, washed with absolute and 70% ethanol, and subsequently digested in lysis buffer (50 mM Tris–HCl, 10 mM EDTA, 150 mM NaCl, 0.5% sodium dodecyl sulfate, and 0.4 mg/L proteinase K) at 55°C overnight. DNA was extracted using a phenol–chloroform extraction-based protocol, followed by ethanol precipitation and re-dissolving in TE buffer. Fresh-frozen tissues were digested in lysis buffer as described earlier at 55°C overnight, 1/100 volume of RNase A

Table 1 Clinical findings in cases of T-cell lymphomas

Disease	Case No.	Age range (mean) years	M:F	Site of involvement (No. of patients)	Past History (No. of patients)
PTCL-NOS	30	50~90 (69)	13:17	LNs (21), stomach (1), colon (1), spleen (2), tonsil (2), bone marrow (1)	SLE (1), Hashimoto thyroiditis (1), HTN (5)
AITL	17	49~82 (68)	12:5	LNs (15), spleen (1)	HTN (1), HCV (1), DM (1)
ATL	13	44~77 (59)	8:5	LNs (8), thyroid (1), tonsil (1), small intestine (1), stomach (2)	n.p.
ALCL	6	37~75 (57.3)	1:2	LNs (5), Ant. chest wall tumor(1)	n.p.
LBL	8	17~32 (24.5)	1:1	LNs (5), tonsil(1), mediastinal, abd. masses	n.p.
ITL	2	59~74 (66.5)	1:1	Small intestinal LN and Ileum	HTN

LNs, lymph nodes; SLE, systemic lupus erythematosus; HCV, hepatitis C virus; HTN, hypertension; DM, diabetes mellitus; Ant, anterior; Abd, abdominal; n.p., not particulary.

(10 mg/mL) was added, the mixture was incubated at 37°C for at least 1 h, and finally DNA was extracted as described earlier.

According to the BIOMED-2 protocol, immunoglobulin (Ig) gene rearrangement was analyzed using eight PCRs with 41 primers: four multiplex PCRs and one single PCR with 28 primers for the Ig heavy chain (IgH) gene (three VH–JH and two DH–JH), two multiplex PCRs with 10 primers for the Ig kappa light chain (IgK) gene, and one multiplex PCR with three primers for the Ig lambda light chain (Igλ) gene. T-cell receptor (TCR) gene rearrangement was analyzed using six PCRs with 56 primers: three multiplex PCRs with 38 primers for the TCR beta (TCRβ) gene, two multiplex PCRs with six primers for the TCR gamma (TCRγ) gene, and one multiplex PCR with 12 primers for the TCR delta (TCRδ) gene. PCR was performed according to the modified BIOMED-2 protocol, as described previously (9). Amplification was initiated by heating at 95°C for 7 min, followed by 40 cycles of 95°C for 30 s, 60°C for 30 s, and 72°C for 30 s, and a final incubation at 72°C for 5 min. Amplified PCR products were electrophoresed in 5.0% or 6.6% polyacrylamide (PAA) gels, based on fragment sizes, stained with ethidium bromide, and then visualized by ultraviolet illumination. To determine the sensitivity limit of PAA gel electrophoresis, we performed a serial dilution experiment by mixing DNA from the monoclonal T-cell line (PEER) with DNA from polyclonal human tonsillar tissue and then adjusting to a final concentration of 60%-6%-0.6% of clonal T-cell DNA. The PEER cell line and polyclonal human tonsillar tissue were also used as monoclonal and polyclonal controls, respectively.

Statistical analyses

Differences in frequencies of occurrence of B-cell clones in different cases and their association with EBV were compared using chi-squared test or Fisher's exact probability test. Survival curves and overall survival rates were calculated using the Kaplan–Meier method and were compared using the log-rank test.

Results

Clonality analysis

Cases yielding smear and oligoclonal bands were defined as polyclonal, and those with single or double bands in more than one primer set or showing bands with identical sizes in duplicate reactions were defined as monoclonal (Fig. 1). Fresh-frozen tissues were available in 14 cases. In these cases, results of the clonality analysis on paraffin-embedded samples and fresh samples were identical. The sensitivity limit of our PAA gel electrophoresis method was more than 6% because a weak monoclonal band could be observed at that concentration.

Clonal rearrangement of TCR and Ig genes was detected in 59 (77.6%) and 14 (18.4%) of 76 cases with T-cell lymphoma, respectively (Table 2).

Peripheral T-cell lymphoma, not otherwise specified

Of the 30 cases studied, 27 (90%) and nine (30%) exhibited clonal rearrangement of TCR and Ig genes, respectively. Among cases with B-cell clones, rearrangement was detected only in the immunoglobulin heavy chain (IgH) gene. Three (33.3%) of nine cases with many scattered large B cells (LBCs) were associated with B-cell clones. Twenty (66.6%) cases had T-cell clones with no Ig gene rearrangement.

Angioimmunoblastic T-cell lymphoma

Of the 17 cases studied, 13 (76.4%) and three (17.6%) exhibited clonal rearrangement of TCR and Ig genes, respectively. Eleven (64.7%) cases had T-cell clones with no Ig gene rearrangement. Four (23.5%) cases failed to show monoclonal bands for T cells, whereas one exhibited monoclonal B cells. One (20%) case of five showed many aggregated LBCs associated with B-cell clones.

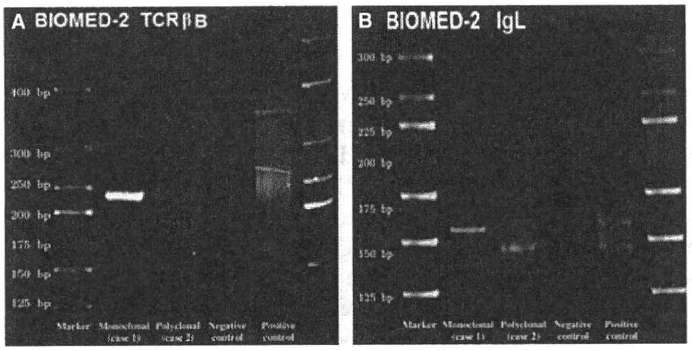

Figure 1 Clonality analysis of two cases of angioimmunoblastic T-cell lymphoma showing the monoclonal (case 1) and polyclonal (case 2) bands of two primer sets detected by TCRβ (Fig. 1A) and IgL (Fig. 1B) genes. Follicular hyperplasia and H_2O were used as positive and negative controls, respectively.

Table 2 Results of clonality analysis in T-cell lymphomas

Disease	Case No.	TCR gene rearrangements				Ig gene rearrangements		
		TCRγ (%)	TCRβ (%)	TCRδ (%)	Total (%)	IgL (%)	IgH (%)	Total (%)
PTCL-NOS	30	24 (80)	12 (40)	7 (23)	27 (90)	0 (0)	9 (30)	9 (30)
AITL	17	13 (76.4)	4 (23.5)	0 (0)	13 (76.4)	2 (12)	3 (17.6)	3 (17.6)
ATL	13	8 (61.5)	8 (61.5)	4 (31)	10 (77)	0 (0)	1 (7.6)	1 (7.6)
ALCL	6	3 (50)	0 (0)	0 (0)	3 (50)	0 (0)	0 (14.2)	0 (0)
T-LBL	8	3 (37.5)	0 (0)	2 (25)	5 (62.5)	0 (0)	1 (12.5)	1 (12.5)
ITL	2	1 (50)	0 (0)	0 (0)	1 (50)	0 (0)	0 (0)	0 (0)
Total	76	52 (68.4)	24 (31.5)	13 (17.1)	59 (77.6)	2 (2.6)	14 (18.4)	14 (18.4)

PTCL-NOS, peripheral T-cell lymphoma; not otherwise specified, AITL, angioimmunoblastic T-cell lymphoma; ATL, adult T-cell lymphoma; ALCL, anaplastic large-cell lymphoma; T-LBL, T-lymphoblastic lymphoma; ITL, intestinal T-cell lymphoma.

Adult T-cell lymphoma

Ten (77%) and one (7.6%) cases exhibited clonal rearrangement of TCR and Ig genes, respectively. In the case with the B-cell clone, Ig gene rearrangement was detected using the incomplete DH–JH primer set: this case was also EBV positive. One (20%) case of five showed few scattered LBCs that were associated with B-cell clones, and the predominant reactive cells were macrophages with epithelioid features.

Anaplastic large-cell lymphoma

Three (50%) of the six ALCL cases exhibited clonal rearrangements of TCR genes without Ig gene rearrangement.

Precursor T-lymphoblastic lymphoma

Five (62.5%) and one (12.5%) of eight cases exhibited clonal rearrangements of TCR and Ig genes, respectively. In two (25%) of the five cases, T-cell clones were detected by TCRδ gene analysis. Four (50%) of eight cases showed a few scattered LBCs with B-cell clones in one.

Intestinal T-cell lymphoma

One of the two ITL cases showed monoclonal rearrangement of TCRγ without concurrent Ig gene rearrangement with a few scattered LBCs observed in both cases.

In situ hybridization

ISH with the EBER probe yielded positive signals in the nucleus. When positive signals were found in more than three per 100 large lymphoid cells, these cases were judged to be EBV positive based on previously used criteria (4, 5). Twenty-one (27.6%) of all PTCL cases were judged as EBV positive: 10 (33.3%) of 30 PTCL-NOS, seven (41%) of 17 AITL, three (23%) of 13 ATL, one (16.6%) of six ALCL, and no T-LBL or ITL cases was EBV positive (Table 3).

Table 3 The correlation between presence of B-cell clones with EBV and large B cells

Disease	Case No.	No. of EBV-positive cases (%)	Large B cells	
			Few	Many
Peripheral T-cell lymphoma, not otherwise specified				
With B-cell clones	9	6 (66.6)	4	3
Without B-cell clones	21	4 (19)	9	5
Angioimmunoblastic T-cell lymphoma				
With B-cell clones	3	2 (66.6)	2	1
Without B-cell clones	14	5 (35.7)	10	4
Adult T-cell lymphoma				
With B-cell clones	1	1 (100)	1	0
Without B-cell clones	12	2 (16.6)	4	0

B-cell clones were detected in six of 10 EBV-positive cases with PTCL-NOS, showing that the appearance of B-cell clones was significantly correlated with EBV positivity ($P < 0.05$). Cases with many scattered/aggregated LBCs showed a higher frequency of EBV positivity than those without among all PTCL cases ($P = 0.001$) and PTCL-NOS cases ($P = 0.04$).

Clonality analysis in serial biopsy cases

Clonality analysis was performed on serially biopsied specimens in two cases (cases 1, 2). A brief clinical course of these cases is described later.

Case 1.

A 59-yr-old woman was initially diagnosed with multiple myeloma in 2005. Three years later, a swollen lymph node (LN) was biopsied and diagnosed as PTCL-NOS. IHC justified the diagnosis of PTCL-NOS with monoclonal B-cell proliferation (Fig. 2A,B). In double staining using EBER ISH and IHC with CD20, EBV-positive cells expressed CD20, indicating that EBV infected LBCs (Fig. 2C). One year later, ulcerative lesions in the ileocecal region were biopsied, revealing a finding similar to the previously biop-

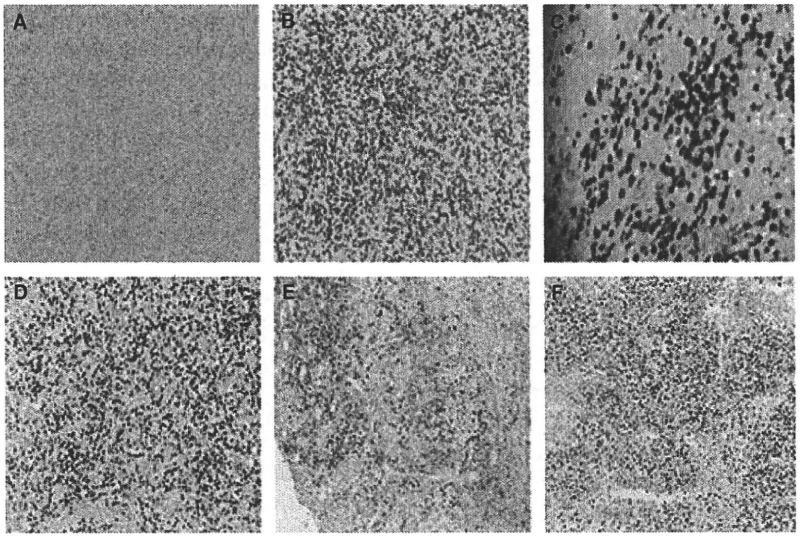

Figure 2 Case 1. Peripheral T-cell lymphoma, not otherwise specified (PTCL-NOS). (A) Diffuse proliferation of medium-to-large lymphoid cells with irregular, hyperchromatic nuclei. Hematoxylin and eosin staining (magnification ×200). (B) Immunohistochemistry with CD3 antibody. Medium-to-large lymphoid cells showing positive staining (magnification ×200). (C) Double staining using *in situ* hybridization (ISH) with the EBER probe and immunohistochemistry with the CD20 antibody. EBV signals were detected in the nuclei of $CD20^+$ cells (magnification ×400). (D) EBV-positive cells in the lymph node (LN) at first biopsy. ISH, magnification ×200. (E) EBV-positive cells were slightly decreased in the colon at the second biopsy. ISH, magnification ×200. (F) EBV-positive cells were increased in the LN at autopsy (C). ISH, magnification ×200.

sied LN, whereas ISH revealed that the EBV-containing cells decreased in number compared with those in the LN (Fig. 2D,E). Clonality analysis revealed a weak monoclonal band in the IgH chain different in size from that in the original LN. Monoclonal proliferation of T cells was not detected. The patient died and an autopsy revealed that proliferating cells in the small and large intestines as well as the para-aortic LN were positive for leukocyte common antigen, but negative for CD3, CD79a, and CD20. ISH revealed that EBV-containing cells were larger in number in the LN and colon at autopsy than in the initially biopsied LN (Fig. 2F).

Case 2.

Clinicopathological findings in this case were reported previously (6). Briefly, a 69-yr-old man presented with LN swelling in the right inguinal region, which was biopsied (LN1) and diagnosed as PTCL. About 51 months after combination chemotherapy, erythematous papules, systemic lymphadenopathy, and a fever of 38°C appeared. Skin (S1) and lymph nodes (LN2) were biopsied. Erythematous papules disappeared spontaneously but reappeared and were biopsied (S2). The patient died 4 months after disease recurrence. LN1 was diagnosed as being $CD3^{\pm}$, $CD4^{\pm}$, and $CD8^-$. In LN2, the large cells with $CD3^{\pm}$, $CD4^{\pm}$, and $CD8^-$ decreased in number, while numerous $CD20^{\pm}$ large cells were discernible. Clonality analysis revealed the persistent presence of an identical T-cell clone in LN1 and LN2. Clonal bands of the IgH chain gene were detected in LN2, but not in LN1. S1 and S2 showed diffuse proliferation of small to large lymphoid cells that were $CD20^-$, $CD3^{\pm}$, $CD4^{\pm}$, and $CD8^-$ in the upper dermis. Clonality analysis revealed the presence of a T-cell clone identical to LN1 and LN2 with no B-cell clone, indicating the recurrence of PTCL. EBV genomes, detected in the nucleus of LBC, appeared only in LN2. Taken together, EBV-positive LBCs appeared transiently during the course of PTCL-NOS.

Clinical findings

Clinicopathological findings in the 76 cases are summarized in Table 1. Among PTCL cases, ages of patients were higher in PTCL-NOS and AITL than in ATL and ALCL cases. Except for PTCL-NOS and ALCL cases, men predominated. Ages of the patients in T-LBL ranged from 17 to 36 (mean, 24.5) yrs with a male/female ratio of 1 : 1. No difference was found between clinical and histopathological findings regarding the presence or absence of B-cell clones except for AITL cases, in which the frequency of patients less than 60 yrs old was higher in cases with B-cell clones than in those without ($P = 0.01$). The LN was the most common site for involvement, except in ITL cases. HTLV-1 was negative except in ATL cases. Most patients received chemotherapy, with three patients receiving radiotherapy. The chemotherapeutic agents used were cyclophosphamide, hydroxydaunorubicin, vincristine, and prednisone with

or without methotrexate in most patients. Complete remission occurred in 14 cases and disease progression in 28 cases. Relapse occurred 2–87 (mean 25.6) months after completion of therapy in 15 of 61 cases for which follow-up data were available.

Histopathological findings

In every case, diffuse proliferation of medium-to-large lymphoid cells was observed with irregular, hyperchromatic nuclei, in which prominent nucleoli were discernible. Varying numbers of inflammatory cells, including small lymphocytes, plasma cells, macrophages, and/or eosinophils, were found, yielding a polymorphous appearance. When arborizing vessels and clusters of medium-to-large cells with voluminous, clear cytoplasm (clear cells) were found, the diagnosis of AITL was made, in which proliferating large lymphoid cells detected by CD10 and PD-1 were occasionally positive and the follicular dendritic cell meshwork expressing CD21 were present in all AITL cases, and they were expanded in most cases. ALCL cases showed relatively cohesive proliferation of large atypical cells with eccentric horseshoe- or kidney-shaped nuclei and rich eosinophilic cytoplasm, which were $CD4^+$, $CD30^+$, $CD20^-$, and $CD3^\pm$. The tumor cells of all ALCL cases showed a strong and equal level of CD30 expression. According to the WHO criteria, these findings met criteria for ALCL. ALK was negative in all but one case. The present series of ALCL contained relatively elderly patients, which may explain the absence of $ALK^\pm$ cases. ATL cases usually exhibited features of PTCL-NOS, but variations in nuclear size and appearance of multilobated nuclei were found frequently, giving a pleomorphic appearance. The tumor cells of ITL were medium to large in size and contained a moderate amount of cytoplasm, in which round nuclei with prominent nucleoli were found. Tumor cells in T-LBL had medium-sized nuclei with stippled chromatin and scant cytoplasm.

LBCs were found in most cases: a few scattered in 41 cases, many scattered in nine, many aggregates in five, and a few aggregates in one (Fig. 3). B-cell clones were detected in four cases with many scattered/aggregated LBCs (Table 3).

Clinical outcome

The follow-up periods for the survivors ranged from 3 to 103 (mean 25.2) months. The Kaplan–Meier estimated survival rate at 3 yr was 47.6%. Considering T-cell lymphomas as a whole and individually, no significant correlation was found between the appearance of LBCs and prognosis. The complete remission rate in cases with LBCs (15%) was lower than that in cases without LBCs (30%), but the difference was not statistically significant.

Discussion

Approximately 200 T-cell lymphoma cases were initially retrieved from the OLSG file for this study using paraffin-embedded samples. However, 76 cases were available for clonality analysis, because the DNA extracted was occasionally of poor quality because of various factors, such as fixatives, thickness of sectioned tissues, and duration of stored times (10–12). Generally, the quality of DNA was good in samples stored for < 2 yr but very poor in those stored for over 15 yr. More than 50% of the selected cases were rejected because of poor-quality samples, most likely because of the following reasons: the cases were registered with various institutions where handling methods of

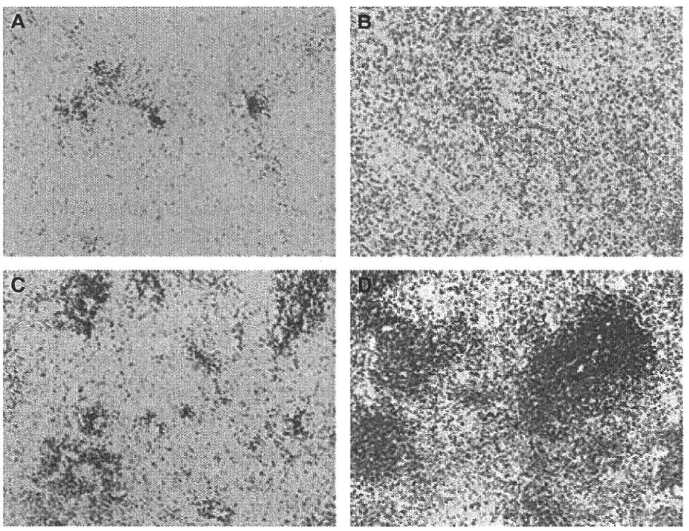

Figure 3 Immunohistochemical staining with CD20 antibody. Large B cells were found as scattered few (A), scattered many (B), aggregated few (C), and aggregated many (D); magnification ×10.

resected specimens varied, samples with storage periods of < 2 yr represented about 8% of cases, and only cases with more than 300 bp of DNA available for analysis were selected to obtain comprehensive results.

In the present series, using the modified BIOMED-2 method on paraffin-embedded specimens, T-cell clones were detected in 59 (77.6%) of 76 cases with T-cell lymphomas, 90% in PTCL-NOS, 76.4% in AITL, 77% in ATL, 50% in ALCL, 62.5% in T-LBL, and 50% in ITL cases. The present findings were generally consistent with those in previous studies, in which T-cell clones were detected in approximately 65–90% of each subtype of PTCL (2, 4, 5). TCR gene rearrangements could not be detected in some of the present cases, possibly because of the relative lower sensitivity of polyacrylamide gel visualization used in our study. T-cell clones were detected primarily in the analysis of TCRγ and/or TCRβ gene rearrangements and less frequently in TCRδ gene arrangement. Analysis of the TCRδ gene is known to be more valuable for detection of T-cell clones in T-cell lymphomas of the immature type (3, 13).

B-cell clones were detected in 14 (18.4%) of 76 cases: nine (30%) PTCL-NOS, three (17.6%) AITL, one (7.6%) ATL, and one (12.5%) T-LBL case. Previous studies have demonstrated simultaneous Ig and TCR gene rearrangements in 10% of lymphoma and leukemia cases (14–16). This indicates the coexistence of B- and T-cell clones in the lesional tissues or a dual genotype in the tumor cells. The dual genotype in tumor cells was described in up to 30% of cases of precursor lymphoid neoplasms, although it occurred rarely in lymphomas with a mature phenotype (17). The present results of Ig and TCR gene rearrangements were found in PTCL cases, suggesting coexistence of B- and T-cell clones, not the dual genotype.

Previous studies have shown that PTCL with B-cell clones showed a worse prognosis than PTCL without B-cell clones (6, 7, 18, 19). In the present cases, PTCL with B-cell clones exhibited a similar prognosis to PTCL without B-cell clones: the 3-yr survival rate was 38.9% and 52.2%, respectively. However, the complete remission rate was lower in cases with B-cell clones (15%) than those without (30%).

The presence of B-cell clones was highly associated with EBV positivity among the PTCL cases as a whole (P = 0.0012) and PTCL-NOS cases (P = 0.0112). However, no significant correlation with EBV was found with other types of PTCL, possibly because of the small number of cases examined. Development of B-cell lymphoma in immunocompromised hosts is well known: escape of EBV latent gene expressing B cells from immune surveillance because of immunodeficiencies is the most likely explanation for this. Taking this into account, the presence of B-cell clones in different types of T-cell lymphomas might be because of the evolution of immunodeficient conditions during the courses of these lymphomas (20, 21). Association of the presence of the EBV genome in LBCs and occurrence of clonal B-cell proliferation found in the present series suggest a role for immunodeficient conditions in clonal B-cell proliferation. Another possible explanation is the ability of B-cell clones to proliferate and expand to clonal cells with the support of cytokines produced by neoplastic T cells (22, 23).

The presence of the EBV genome in the lesional tissues of T-cell lymphomas was reported to be in 31–57% of cases (19, 24–26), although *in situ* localization of the EBV genome was not strictly defined to a specific kind of cell (i.e. neoplastic T cells or possibly intermingled LBCs). The present findings of double staining in which the EBV genome was present in $CD20^+$ B cells but not in $CD3^+$ T cells in the lesional tissues of T-cell lymphomas prompted us to re-evaluate EBV positivity in T-cell lymphomas. From the histopathological and immunohistochemical findings, together with results of double staining in a limited number of cases, EBV seemed to be confined to LBCs.

Information regarding serial biopsies was available in two of the present cases (i.e. cases 1 and 2). Appearance of EBV-positive cells was persistent or rather increased during the 1-yr course of case 1 but was transient during the 4-month course of case 2. Further analysis is necessary to evaluate the pathological significance of the presence of EBV-positive LBCs in PTCL. At a minimum, careful follow-up is recommended for an appropriate selection of therapeutic modalities.

In conclusion, B-cell clones were occasionally present in cases of T-cell lymphoma, with close association of the appearance of LBCs with the EBV genome in the lesions, suggesting a causal link between EBV and B-cell proliferation. The response to chemotherapy was worse in cases with B-cell clones than in those without. EBV-positive B cells might persist or disappear during the disease course. Factors affecting the change of EBV-positive B cells have yet to be clarified.

Acknowledgements

We thank Ms. T. Sawamura, M. Sugano, M. Tone, and E. Maeno for their technical assistance.

References

1. Rodriguez-Abreu D, Filho VB, Zucca E. Peripheral T-cell lymphomas, unspecified (or not otherwise specified): a review. *Hematol Oncol* 2008;**26**:8–20.
2. Brüggemann M, White H, Gaulard P, *et al.* Powerful strategy for polymerase chain reaction-based clonality assessment in T-cell malignancies. Report of the BIOMED-2 Concerted Action BHM4 CT98-3936. *Leukemia* 2007;**21**:215–21.

3. van Dongen JJ, Langerak AW, Brüggemann M, *et al.* Design and standardization of PCR primers and protocols for detection of clonal immunoglobulin and T-cell receptor gene recombination in suspect lymphoproliferations: report of the BIOMED-2 Concerted Action BMH4-CT98-3936. *Leukemia* 2003;**17**:2257–317.
4. Tan BT, Seo K, Warnke RA, Arber DA. The frequency of immunoglobulin heavy chain gene and T-cell receptor gamma-chain gene rearrangements and Epstein–Barr virus in ALK+ and ALK- anaplastic large cell lymphoma and other peripheral T-cell lymphomas. *J Mol Diagn* 2008;**10**:502–12.
5. Tan BT, Warnke RA, Arber DA. The frequency of B- and T-cell gene rearrangements and Epstein-Barr virus in T-cell lymphomas: a comparison between angioimmunoblastic T-cell lymphoma and peripheral T-cell lymphoma, unspecified with and without associated B-cell proliferations. *J Mol Diagn* 2006;**8**:466–75.
6. Chihara T, Wada N, Kohara M, *et al.* Peripheral T-cell lymphoma of Lennert type complicated by monoclonal proliferation of large B-cells. *Pathol Res Pract* 2010;**206**:185–90.
7. Higgins JP, van deRijn M, Jones CD, Zehnder JL, Warnke RA. Peripheral T-cell lymphoma complicated by a proliferation of large B cells. *Am J Clin Pathol* 2000;**114**:236–47.
8. Willenbrock K, Bräuninger A, Hansmann ML. Frequent occurrence of B-cell lymphomas in angioimmunoblastic T-cell lymphoma and proliferation of Epstein-Barr virus-infected cells in early cases. *Br J Haematol* 2007;**138**:733–9.
9. Wada N, Ikeda J, Kohara M, *et al.* Diffuse large B-cell lymphoma with a high number of epithelioid histiocytes (lymphoepithelioid B-cell lymphoma): a study of Osaka Lymphoma Study Group. *Virchows Arch* 2009;**455**:285–93.
10. Sato Y, Sugie R, Tsuchiya B, Kameya T, Natori M, Mukai K. Comparison of the DNA extraction methods for polymerase chain reaction amplification from formalin-fixed and paraffin-embedded tissues. *Diagn Mol Pathol* 2001;**10**:265–71.
11. Bagg A, Braziel RM, Arber DA, Bijwaard KE, Chu AY. Immunoglobulin heavy chain gene analysis in lymphomas. A multi-center study demonstrating the heterogeneity of performance of polymerase chain reaction assays. *J Mol Diagn* 2002;**4**:81–9.
12. Alaibac M, Filotico R, Giannella C, Paradiso A, Labriola A, Marzullo F. The effect of fixation type on DNA extracted from paraffin-embedded tissue for PCR studies in dermatopathology. *Dermatol* 1997;**195**:105–7.
13. Van Krieken JH, Elwood L, Andrade RE, Jaffe ES, Cossman J, Medeiros LJ. Rearrangement of the T-cell receptor delta chain gene in T-cell lymphomas with a mature phenotype. *Am J Pathol* 1991;**139**:161–8.
14. Pelicci P-G, Knowles DM II, Dalla Favera R. Lymphoid tumors displaying rearrangements of both immunoglobulin and T cell receptor genes. *J Exp Med* 1985;**162**:1015–24.
15. Smith JL, Hodges E, Quin CT, McCarthy KP, Wright DH. Frequent T and B cell oligoclones in histologically and immunophenotypically characterized angioimmunoblastic lymphadenopathy. *Am J Pathol* 2000;**156**:661–9.
16. Yao L, Chen Z, Cen J, Liang J, Feng Y, He J, Qi X, Shen H. The pattern of clonal immunoglobulin and T-cell receptor (Ig/TCR) gene rearrangements in Chinese adult acute lymphoblastic leukemia patients. *Leuk Res* 2008;**32**:1735–40.
17. Williams ME, Innes DJ Jr, Borowitz MJ, Lovell MA, Swerdlow SH, Hurtubise PE, Brynes RK, Chan WC, Byrne GE Jr, Whitcomb CC. Immunoglobulin and T cell receptor gene rearrangements in human lymphoma and leukemia. *Blood* 1987;**69**:79–86.
18. Dupuis J, Emile JF, Mounier N, *et al.* Prognostic significance of Epstein–Barr virus in nodal peripheral T-cell lymphoma, unspecified: A Groupe d'Etude des Lymphomes de l'Adulte (GELA) study. *Blood* 2006;**15**: 108.
19. Zettl A, Lee SS, Rüdiger T, Starostik P, Marino M, Kirchner T, Ott M, Müller-Hermelink HK, Ott G. Epstein-Barr virus-associated B-cell lymphoproliferative disorders in angioimmunoblastic T-cell lymphoma and peripheral T-cell lymphoma, unspecified. *Am J Clin Pathol* 2002;**117**:368–79.
20. Anagnostopoulos I, Hummel M, Finn T, Tiemann M, Korbjuhn P, Dimmler C, Gatter K, Dallenbach F, Parwaresch MR, Stein H. Heterogeneous Epstein–Barr virus infection patterns in peripheral T-cell lymphoma of angioimmunoblastic lymphadenopathy type. *Blood* 1992;**80**:1804–12.
21. Weiss LM, Jaffe ES, Liu XF, Chen YY, Shibata D, Medeiros LJ. Detection and localisation of Epstein–Barr viral genomes in angioimmunoblastic lymphoadenopathy and angioimmunoblastic lymphadenopathy-like lymphoma. *Blood* 1992;**79**:1789–95.
22. Foss HD, Anagnostopoulos I, Herbst H, Grebe M, Ziemann K, Hummel M, Stein H. Pattern of cytokine gene expression in peripheral T-cell lymphoma of angioimmunoblastic lymphadenopathy type. *Blood* 1995;**85**:2862–9.
23. Merz H, Fliedner A, Orscheschek K, Binder T, Sebald W, Müller-Hermelink HK, Feller AC. Cytokine expression in T-cell lymphomas and Hodgkin's disease: its possible implication in autocrine or paracrine production as a potential basis for neoplastic growth. *Am J Pathol* 1991;**139**:1173–80.
24. Hamilton-Dutoit SJ, Pallesen G. A survey of Epstein–Barr virus gene expression in sporadic non-Hodgkin's lymphomas: detection of Epstein–Barr virus in a subset of peripheral T-cell lymphomas. *Am J Pathol* 1992;**140**:1315–25.
25. Korbjuhn P, Anagnostopoulos I, Hummel M, Tiemann M, Dallenbach F, Parwaresch MR, Stein H. Frequent latent Epstein–Barr virus infection of neoplastic T cells and bystander B cells in human immunodeficiency virus-negative European peripheral pleomorphic T-cell lymphomas. *Blood* 1993;**82**:217–23.
26. Ott G, Ott MM, Feller AC, Seidl S, Muller-Hermelink HK. Prevalence of Epstein–Barr virus DNA in different T-cell lymphoma entities in a European population. *Int J Cancer* 1992;**51**:562–7.

